Realization of a Cognitive Radio-Mesh Network Based on OFDMA Technology

Realization of a Cognitive Radio-Mesh Network Based on OFDMA Technology

By

Lili Jiang, B.Sc., M.S.E.E.

A Thesis
Submitted to the School of Graduate Studies
in Partial Fulfilment of the Requirements
for the Degree
Master of Applied Science

McMaster University

MASTER OF APPLIED SCIENCE (2005) McMaster University
(Electrical and Computer Engineering) Hamilton, Ontario

TITLE: Realization of a Cognitive Radio-Mesh Network Based on OFDMA Technology

AUTHOR: Lili Jiang, B.Sc., M.S.E.E.

SUPERVISOR: Prof. Simon Haykin

NUMBER OF PAGES: — xiv, 96

Abstract

The goal of this thesis is to realize some critical techniques required in the cognitive radio mesh network. Cognitive radio (CR) is a new technology introduced to improve the frequency efficiency of current wireless systems. A mesh network, which leverages the advantages of an infrastructure network and a pure ad-hoc network, is a network topology highly suitable for the CR networks. CR users need to adapt to their ambient wireless environment and automatically select their own effective transceiver mode.

The thesis focuses on the realization of a physical layer protocol, dynamic frequency-selection algorithm, mesh network signalling method, and transmit-power control algorithm in CR mesh networks. A new dynamic frequency selection algorithm is introduced in CR network, including estimation of the primary users' traffic statistics as well as adaptation to the local background noise interference. Through continuous observation, analysis, and adaptation to the time-varying environment, CR is able to select the candidate frequency bands to satisfy a user's rate and power requirements without causing collision to the primary users in those bands. As a generic model, a Gaussian mixture model, is selected for characterizing the statistics of the traffic environment.

The transmit-power control in the CR mesh network is based on an iterative water-filling algorithm, rooted in information theory. The iterative water-filling algorithm is modified to suit the requirement of CR mesh networks. It works well for setting a suitable transmit-power level, sub-channels, and sub-carriers for the nodes in a CR mesh network.

To support current systems, experiments are presented on the wireless mesh network, which are based on the orthogonal frequency-division multiple-access (OFDMA) mode of the High-speed Unlicensed Wireless Metropolitan Area Network (Wireless HU-

MAN). In the mesh network, the multiple access control(MAC) layer signals including the distributed network configuration, network entry, and network scheduling signals, are introduced. They are transmitted through a control channel in a cooperative mechanism. The physical layer(PHY) of OFDMA is also discussed in the thesis.

Acknowledgements

First and foremost, I am greatly indebted to my supervisor, Dr. Simon Haykin, for his support and guidance to my research. During my stay in McMaster, I have been deeply impressed by his hard work and endless enthusiasm in the pursuit of scientific knowledge. He contributes in a variety of academic topics. It is a great period in my life to study and work under the supervision of Dr. Haykin.

I own my deepest gratitude and appreciation to my parents and my sisters for their endless and unselfish support, love, patience, and understanding. No matter what happens, they are always there when I need them.

I would like to thank Dr. Zhao for discussions and her guidance of my research. I must also thank Cosmin Coroiu and Terry Greenlay for their assistance in computer facilities and other matters. Special thanks must go to Lola Brooks, Cheryl Gies, and Helen Jachna for their countless helps and supports throughout my study.

Many thanks also go to Kris Huber, Nikita A. Visnevski, Nelson Costa, Tao Feng, Kevin Zhang, Karl Wiklund, and Zhe Chen, for helpful discussions and feedbacks on my research. I also thank Yanwu Ding, Rong Dong, and Hongyan Liu for their help and fun together during my stay in McMaster.

Last but by no means least, I thank my dear daughter Ellen He. She gives me a lot of fun in my life.

I dedicate this work to my parents

Table of Contents

List of Figures

List of Tables

Acronyms

BS: Base Station

CR: Cognitive Radio

CSMA/CA: Carrier-Sensing Multiple Access/Collision Avoidance

DBTMA: Dual Busy Tone Multiple Access

DCA: Dynamic Channel Allocation

DFS: Dynamic Frequency Selection

FFT: Fast Fourier Transform

GMM: Gaussian Mixture Model

HUMAN: High-speed Unlicensed Metropolitan Area Network

ICI: Inter-Channel Interference

IWF: Iterative Water-Filling

MAC: Multiple Access Control

MSH-NCFG: Mesh Network Configuration

MSH-NENT: Mesh Network Entry

MSH-DSCH: Mesh Distributed Scheduling

OFDMA: Orthogonal Frequency Division Multiple Access

PHY: Physical layer

PMP: Point-to-Multi-Point

QAM: Quadrature Amplitude Modulation

RSS: Receive Signal Strength

SINR: Signal-to-Interference-Noise Ratio

SNR: Signal-to-Noise Ratio

SS: Subscriber Station

TPC: Transmit-Power Control

WLAN: Wireless Local Area Network

WMAN: Wireless Metropolitan Area Network

ZRP: Zero Routing Protocol

Chapter 1

INTRODUCTION

1.1 Cognitive Radio and Its Critical Technologies

The world of communications is a dynamic and rapidly changing arena in which technology is constantly evolving. Wireless communication permeates in every corner of the world, and changes our daily lives profoundly. During the past few decades, communication technology has changed rapidly from analog to digital and from hardware to software. Today, inexpensive chips with millions of transistors, new modulation techniques and our own better understanding of information theory, let us embed powerful signal processing into transmitters and receivers. It is possible for them to discern desired signals from possibly many other signals and noise sources. The evolution of radios can be roughly described in three stages(Fette 2003a)(Fette 2003b):

1. Hardware driven radios: In this stage, all radio features, such as the transmission frequency, the modulation type and other RF parameters were determined by system hardware.

2. Digital radios: In this stage, part of the signal processing and transmission were realized digitally, such as using embedded DSP. However, digital radios cannot be programmed in the field.

3. Software defined radios: In software defined radios, all functions, modes, waveform properties, cryptography and applications can be configured and reconfigured by software.

As a result of the flexibility of software defined radio, Cognitive Radio (CR), a new generation of wireless communication, is the path toward which computer-control systems and telecommunication techniques are migrating.

CR is a self-managing system(Cowen-Hirsch 2000) that can configure and reconfigure itself. In (Haykin 2005), Haykin described CR as a "Brain-empowered wireless communication". He outlined CR in six key words: awareness, intelligence, learning, adaptivity, reliability, and efficiency. According to a 2002 FCC report(FCC 2002), the spectrum shortage is artificial; the bottleneck is not the spectrum itself, but the access techniques used in radios. However, radio spectrum technology and regulatory policy are currently in the midst of a revolution. CR is expected to deal intelligently with the radio environment. This new technique can avoid the crowded bands, and choose the best suited protocol for the selected frequency bands.

Cognitive radio makes the spectrum utilization more efficient. Mitola described CR in his PhD thesis as a framework that keeps observing the radio environment, assessing alternatives, generating plans, supervising multimedia services, and learning from its experience(Mitola 2000). This constitutes an observe-think-act cycle(Mitola 1999). CR could select not only the center frequency, but also the bandwidth to satisfy its connection requirement.

The wireless environment is complicated and time varying. Primary users work at their allocated bands and transmit according to their own traffic patterns. To co-exist with primary users, CR users have to adapt to the environment and select their own effective transceiver mode accordingly.

A wireless mesh network is a self-organized flexible network. Its characteristics are well suited for the CR scenario. To analyze CR behavior under realistic conditions in the thesis, our CR analysis is based on the wireless metropolitan network with mesh network topology. Some of the critical techniques in CR, including physical layer realization, dynamic frequency selection and transmit power control, are based on this application background.

For the dynamic frequency selection algorithm by continuous observation, analysis, and adaptation to the time varying environment, CR is able to select an efficient transmit mode to satisfy its own quality of service requirements. Wireless communication provides different kinds of services from radio, television, to cellular phone services and interactive handhold games. Because of this diversity, the traffic patterns of wireless communication systems include a wide range of traffic properties. Like personal switch telecommunication networks, the wireless traffic is usually modeled using a Poisson process. However, in many cases such as wireless local area network (WLAN) traffic model, many papers have shown that this simplified traffic model may not represent real-life data.

In our simulation, we set different traffic patterns for the primary users. On the CR side, the measurement-based traffic analysis does not assume anything about the traffic pattern of the primary users. The dynamic frequency band allocation algorithm of CR makes its decisions based on the traffic statistics of the measured environment. To analyze different traffic patterns under the same umbrella, a Gaussian mixture model (GMM)(Mclachlan and Basford 1992) is used here for characterizing the traffic environment. GMM is a generic model that can cover a variety of traffic modes. In operation, the parameters of the GMM are acquired through online learning by the CR users. This is rather suitable for the wireless environment, which varies with time, frequency, and space. With hands-on knowledge of the environment, the CR system could co-exist with primary users in an adaptive fashion.

The mesh network signalling is realized in the CR. The radio nodes cooperate in a distributed scheduling manner so as to share spectrum and create useful network services. They work cooperatively for the entry of new nodes, for choosing the network configuration, scheduling, spectrum management, and transmit-power control. These concepts are important for building an adaptive, self-organizing wireless network with cross-layer PHY/MAC/network cooperation among CRs.

To save transmit power and reduce interference to other links, the transmit-power control algorithm in CR is based on iterative water-filling in the mesh network. The state transition and performance analysis are detailed in this thesis.

The organization of the thesis is as follows. Chapter 1 is an overview of cognitive radio, the mesh network and 802.16a OFDMA method. Chapter 2 discusses the realization of a mesh network, including physical layer and MAC layer signaling. Chapter 3 discusses the dynamic frequency selection algorithm. Chapter 4 describes the transmit-power control algorithm and the application of iterative water-filling algorithm in cognitive radio network, and Chapter 5 concludes the thesis.

1.2 Mesh Networks

Mesh networks and ad hoc networks are currently under considerable research around the world, both in academia and industry. Depending on whether or not there is a fixed infrastructure, wireless systems can be categorized as infrastructure systems or ad hoc networks. Currently, the legacy networks such as the cellular networks, usually work under the infrastructure mode in a point-to-multi-point(PMP) topology. In the infrastructure system, there are base stations(BS) or access points to perform central administration for multiple subscriber stations(SS). The infrastructure system is organized in cells around BS or access point for channel reuse to increase the spectrum usage. In each cell, the SSs communicate with and only with the BS or access point in that cell which forms a PMP topology.

Compared with the PMP network, an ad hoc network is best suited for environments where infrastructure is unavailable, for example, in hostile environments or rescue scenarios where local infrastructure has been destroyed. In IEEE 802.11 specification, an ad hoc network is described as *a network composed solely of stations within mutual communication range of each other.* In other literatures, ad hoc refers to multi-hop self-configuring wireless networks. An ad hoc network can take on different topologies and can be mobile, stand alone, or networked(Marsic 2003). It is a totally non-infrastructured and self-organized network, with all stations in the network having similar functionality. The stations in ad hoc network are called nodes. A node can build links to transmit to and receive from other nodes directly in the ad hoc network. Packets may need to traverse multiple links to reach their destinations.

Between the two cases of the PMP network and the ad hoc network, there is the wireless mesh network. A mesh network involves the combination of infrastructure mesh and client mesh in (Akyildiz, Wang, and Wang 2005). Compared with infrastructure systems, a mesh network is *more self-organized and distributed, and the subscriber stations can connect and communicate with each other without going through a base station.* However, compared with pure ad hoc networks, the stations in a mesh network may not all have the same functionality. There exist some super-nodes, called the mesh BS, in the system. Most traffic in the mesh network goes to or comes from the mesh BS. Since mesh BSs occupy central positions in their neighborhood, they make the system robust and resilient to faults. With these mesh BSs, mesh network can grow organically. As a hybrid version of the infrastructure system and the pure ad hoc network, a mesh network is more flexible and its protocols are roughly the same as those in the ad hoc network while taking advantage of the mesh BS nodes. The main difference between a wireless mesh network and an ad hoc network is perhaps the traffic pattern. In a mesh network, almost all the traffic goes to or from the mesh BS; while in an ad hoc network, the traffic flows between arbitrary pairs of nodes.

Both cognitive radios and mesh networks are intelligent ways of utilizing the spectrum.

The embedded intelligence will allow each open spectrum CR device to potentially be not only an end node in a network, but also a relay unit for nearby neighbors. They form a mesh network instead of a conventional ad-hoc or PMP architecture(Busch and Malhotra 2002). The FCC also believes that cognitive radio technologies have the "potential to overcome some of the incompatibilities that exist between various communication services both domestically and worldwide."(FCC 2003). Mesh network could cover both PMP and ad hoc network. So the CR should be built on a mesh network.

From the topology point of view, mesh networks have been applied to commercial applications for a long time. Examples of wireless mesh networks can be an enterprise-wide backbone wireless network of access points or a cellular mesh of BSs. Technical results derived from ad hoc networks have helped push the mesh idea from a backbone mesh all the way down to SSs. The characteristics of a mesh network are (Marsic 2003):

- The mesh network organizes and scales more nicely than ad hoc network.
- Infrastructure is not necessary in a mesh network.
- The mesh network is robust and resilient to faults.
- It is a self-managing and self-administering network.
- With relay mechanism, achieving identity and security is a challenge.

A layering model is the most common way to divide a protocol suite to subparts and describe them individually. The seven-layer model was introduced by the International Organization for Standardization more than 20 years ago and is still widely used. According to ISO OSI reference architecture, the communication process is divided into seven layers as shown in Table 1.1(Stallings 2004).

Layer	Responsibilities
Physical	Establishes, maintains and terminates point to point data links
Data Link	Logical link and medium access control
Network	Establishes, maintains and terminates end to end communication
Transport	Ensures reliable end to end network communication
Session	Establishes, maintains and terminates node to node communication
Presentation	Provides network communication services
Application	Provides services to user applications

Table 1.1: ISO OSI seven layers

The widely applied TCP/IP protocol suite is divided into four layers as in Table 1.2(Stallings 2004).

Layer	Responsibilities
Network access	Establishes direct connection to physical medium and handle data flow control
Internet	Establishes, maintains and terminates end to end network communication
Transport	Provides a delivery service for the application layer
Application	Provides application access to communication environment

Table 1.2: TCP/IP four layers

Our discussions focus mainly on the two lower layers: physical layer and data link layer.

1.2.1 Routing algorithms

In a PMP network, traffic always happens between BS and SS, there is no routing requirement. Each SS just needs to associate to a BS. However, routing is an important part in ad hoc networks. A terminal in the ad hoc network can dynamically join or leave the network. Within the network, it can be the role of an information source, data sink, or act as a relay node. Since the wireless àd hoc network is created and organized in a decentralized way, how a node finds and connects to the other terminals becomes an essential module in the ad hoc network. In a mesh network, routing is required among mesh BSs and SSs. The association of an SS to a BS is similar to that in a PMP network, and the routing follows that in an ad hoc network. Several different routing algorithms for ad-hoc network have been proposed and are mainly divided into two main categories: 1. proactive or table-driven routing algorithms(Johnson and Maltz 1996); 2. reactive or on-demand routing algorithms(Schollmeier, Gruber, and Finkenzeller 2002).

Using the proactive routing algorithm, a node has to store the full network view at every time, and all topology updates should be broadcast immediately or with small delay to all the other nodes in the ad hoc network. This character of the proactive algorithm makes routing very fast. However, as the number of nodes increases, the network topology updates so often that the proactive routing algorithm is not feasible for large-scale networks. In contrast to the proactive routing algorithm, the reactive routing algorithm sends the route request through the network only if it needs to setup a link. It prolongs the route setup procedure, but avoids the problems associated with maintaining a global routing table.

The routing algorithm used in the thesis is a zero-routing protocol(ZRP)(Pearlman and Haas 1999). This protocol is a hybrid version of the proactive and reactive algorithms. The ZRP maintains the routing information for a local neighborhood and establishes the route on demand for the destination node beyond its local zone. The advantage of this protocol is that the combination of the proactive and reactive algorithm makes it a compromise solution for the route signal transmission in the network. However, the ZRP routing algorithm is more complicated than proactive routing like destination sequenced distance vector routing and reactive routing like ad hoc on-demand distance vector routing.

1.2.2 Medium access control

Due to the large span and low transmit power of ad hoc networks, multi-hop routing is usually used. Many current ad hoc networks work in a single frequency channel. Some multi-channel ad-hoc networks use a single channel for the control channel and multiple channels for the data traffic with spatial channel reuse(Li, Haas, Sheng, and Chen 2003)(Liu, Li, yu Huang, and Fukuda 2002). All the data channels are shared by a number of communicating nodes in close proximity. The throughput of such a network highly depends on the MAC protocol in use(Haas and Deng 2002). MAC layer protocol controls and coordinates the access to the shared channel by the nodes.

The most common MAC layer protocol in the wireless networks is carrier-sensing multiple access/collision avoidance(CSMA/CA)(Colvin 1983). However, the hidden and exposed nodes phenomenon cannot be avoided in the CSMA/CA protocol. This phenomenon is shown in Figure 1.1.

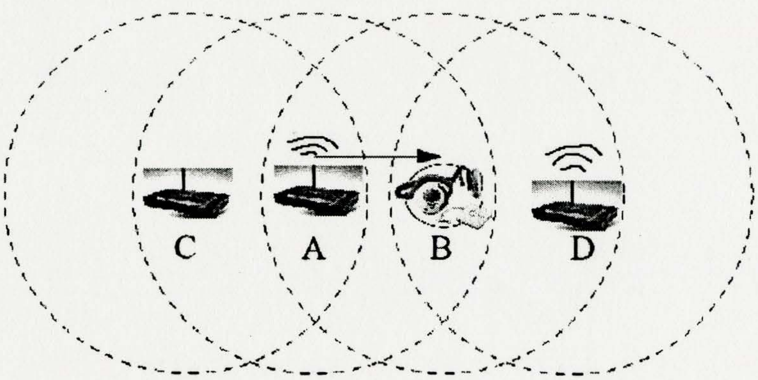

Figure 1.1: Hidden and exposed nodes in ad hoc network

When the transmission happens from node A to node B, hidden nodes are the nodes in the range of the receiver but out of the range of the transmitter as node D, while the exposed nodes are those in the range of the transmitter but out of that in the receiver as node C. The hidden and exposed node issue affects the network capacity. The hidden terminal problem may cause increased collision, while the exposed terminal problem unnecessarily defers nodes from transmitting.
Several attempts at solving the hidden and exposed node issue are found in the literature(Karn 1990)(Bharghavan, Demers, Shenker, and Zhang 1994)(Haas and Deng 2002)(Perkins 2001). Among them, Dual Busy Tone Multiple Access (DBTMA) scheme(Haas and Deng 2002) uses both the require-to-send packet and two out-of-band busy tones to notify neighbor nodes of the channel status. It completely solved the hidden terminal problems and the exposed terminal problems. In our CR mesh network, the use of OFDMA makes it possible to use the DBTMA MAC method. In the thesis, we allocate part of pilot tones to the role of the busy tones in DBTMA algorithm.

1.2.3 Capacity of mesh networks

The ad-hoc network is self organized and each node is independent, so it is not easy to facilitate network management tasks like authorization, authentication and accounting or quality of service features.(Schollmeier, Gruber, and Finkenzeller 2002). Complicated Routing and MAC layer in ad hoc networks requires massive control signalling, which is the overhead of the system and decreases channel capacity for useful payload. Although in ad hoc networks, the transmit power is reduced by the short coverage, the high signalling overhead reduces network capacity as the size of the network grows. As a result, the capacity of the ad hoc network is not that encouraging as we might hope. According to (Gupta and Kumar 2000), for stationary networks, the capacity for each node decreases as $O(1/\sqrt{n})$ with the number of hops n. With existing MAC protocols, measurement in static networks shows the throughput declining even worse with n than theoretically predicted(Gupta and Kumar 2001). While for mobile networks(Grossglauser and Tse 2002), if long delays are tolerated, the capacity may remain constant that is independent of the number of nodes.

In a fully connected mesh network, each node has a connection with all the other nodes. Usually the mesh network is partially connected, designed for the link connection-oriented. Research results have shown that in a wireless mesh network, the throughput of each node decreases as $O(1/n)$, where n is the total number of nodes connected to a mesh BS(Jun and Sichitiu 2003). The mesh BSs then act as bottlenecks in the system. However, this result may be too pessimitic. The wireless mesh network has certain advantages over the ad hoc network. With the unbalanced structure of considerably less powerful SSs, powerful mesh BSs, improved reliability, suitable physical layer adaptation, and probably a lower delay, a wireless mesh network has the potential to increase the bandwidth(Jun and Sichitiu 2003).

1.3 An Overview of 802.16

Due to technological advances in recent years, ad hoc and wireless mesh networks have attracted great attention from industry and have been included in several industrial standards(IEEE802.11 1999)(IEEE802.16 2003)(Medidi and Daptardar 2004)(Nynamics 2004)(Nokia 2002)(Ritter, Friday, Garces, Filippo, Nguyen, and Srivastava). Our CR mesh network is built based on the IEEE 802.16a specification.

The wireless metropolitan area network (WMAN) standard 802.16 is designed for the fixed wireless last-mile connections, and is the wireless counterpart for the cable modem or digital subscribe line(Fong and et. al. 2004). It is a broadband wireless access solution.

As an amendment of 802.16, 802.16a covers the medium access control modifications and additional physical layer specifications for 2-11 GHz. 802.16a works in a none-line-of-sight environment with the maximum coverage of up to 30km. 802.16a can work in the following modes shown in Table 1.3.

Designation	Applicability	Duplexing alternative
WirelessMAN-SCa	2-11 GHz Licensed bands	TDD, FDD
WirelessMAN-OFDM	2-11 GHz Licensed bands	TDD, FDD
WirelessMAN-OFDMA	2-11 GHz Licensed bands	TDD, FDD
WirelessHUMAN	2-11 GHz License-exempt bands	TDD

Table 1.3: Working modes of 802.16a

Here WirelessHUMAN represents the high-speed unlicensed metropolitan area network. For the license-exempt frequency bands between 2 and 11 GHz(primarily 5-6 GHz), WirelessHUMAN should comply with the other three modes. It should further comply with Dynamic Frequency Selection(DFS) protocols. DFS allows the transmitter and receiver to switch to different physical RF channels based on the channel measurement criteria.

The network of 802.16a includes both the PMP network and mesh network topologies. For the PMP, all the traffics occur between the base station(BS) and the subscriber stations(SSs). In the mesh mode, the traffics can be routed through other SSs or occur directly between SSs. The traffic scheduling can be distributed, centralized, or the combination of both.

Since CR users need to co-exist with primary users, multi-tone modulation method can be a good choice so that the primary user bands can be protected while the broadband communication of CR users can guarantee their data rate requirement. In the thesis, the physical layer of CR mesh network is based on WirelessHUMAN-OFDMA operation mode of 802.16a and the mesh signalling is based on the requirement of 802.16a mesh topology requirement.

1.4 Develop tools in CR mesh network

The development of our CR network is based on MATLAB/Simulink and C language in Visual-studio platform. MATLAB is widely used in academia and industry. The emphasis of MATLAB on vector mathematics makes it well suited for communication and digital signal processing. C language is one of the most popular languages used today. It is fast and widely supported. Algorithms developed by C can be easily ported to different hardware platforms.

Simulink is able to scale up simulations to the system-level design(Jiang, Wiklund, and Haykin 2005). With those powerful blocksets provided by Simulink, we can build a CR mesh network frame and integrated detailed algorithms step by step. Algorithms developed in C and MATLAB can be built into Simulink block with Simulink S-functions and integrated in the simulation system.

Summary

In this chapter, we described the cognitive radio concept, and discussed mesh network topology, routing, and medium access techniques. We also illustrated that cognitive radio and mesh topology fit each other rather well. Then we introduced the platform IEEE802.16a, which is used in our CR mesh network simulation. Finally, we talked about the tools used in the CR mesh network development.

Chapter 2

The Mesh Network Realization

The volume and speed of wireless applications will grow faster than the core infrastructure technology is able to support(Akyildiz, Wang, and Wang 2005). At the same time, with ever-increasing data traffic, congestion and bad coverage will become major problems for wireless networks. Novel mesh network architectures that leverage the advantages of an infrastructure network and a pure ad-hoc network, may become the network of choice.

A mesh network is a topology that provides multiple paths between network nodes. A wireless mesh network makes sense since wireless nodes can be easier to connect to other nodes without additional cost, like cables in a wired network. As long as one or more nodes can access the backbone, any node that can connect to any other node of the mesh could get their data to and from the backbone as well. Figures 2.1 and 2.2 show the topologies of point-to-multi-point (PMP) and mesh network.

A wireless mesh network can be realized equally using distributed scheduling, or with the superiority of the mesh BS to realize centralized scheduling. Mesh BS is usually the node with internet backhaul service or has superior computational capability and resources. All the other nodes in the mesh network are called SSs.

In a wireless mesh network, a node's neighbors are the nodes within one-hop of it, and the extended neighborhood of it contains all the nodes within a two-hop area. Figure 2.3 shows the neighbors (within the black contour) and extended neighbors

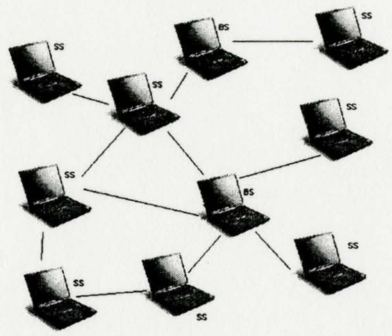

Figure 2.1: The topology of mesh network

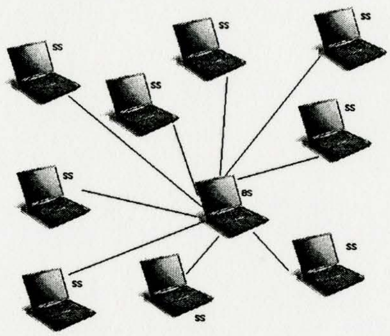

Figure 2.2: The topology of PMP network

(covered by the gray contours) of mesh node 45.

In a mesh network, the transmission works in a coordinated way:
For centralized scheduling, the wireless resources are managed by the mesh BS.
For distributed scheduling, a node must coordinate itself within its extended neighborhood and broadcast its scheduling within that neighborhood.

2.1 Signaling in a Mesh Network

In our CR mesh network simulation, we illustrate the signalling exchange in a mesh network. The signalling exchange procedures will be used in the MAC algorithms of

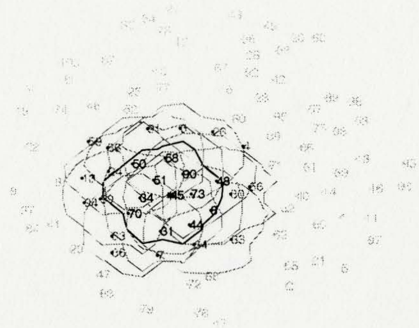

Figure 2.3: The neighborhood of mesh network

dynamic frequency selection and transmit-power control. The wireless mesh network is set up as in Figure 2.3. CRs are the nodes in the mesh network, and they cooperate as well as compete with each other for radio resources. In a mesh network, a node may stay in one of the following states as illustrated in Figure 2.4.
To guarantee that all nearby nodes could receive control channel information, the control channel is circulated through the available channels in the frequency band based on the frame number(IEEE802.16 2003).

Network configuration and network entry packets are two basic packets communicated among nodes. They support the functions of the mesh network, for example, network synchronization, coordination of the channel usage, discovery and network entry of new nodes. Whenever a new node is enabled to enter the mesh network, it goes through the entry procedure. The node entry procedure is realized by a signalling called mesh-network-entry (MSH-NENT). In this period, the new node is called a candidate node. It needs to find an active node in the mesh network called a sponsor candidate for its network connection. The sponsor candidate must have the following characteristics:

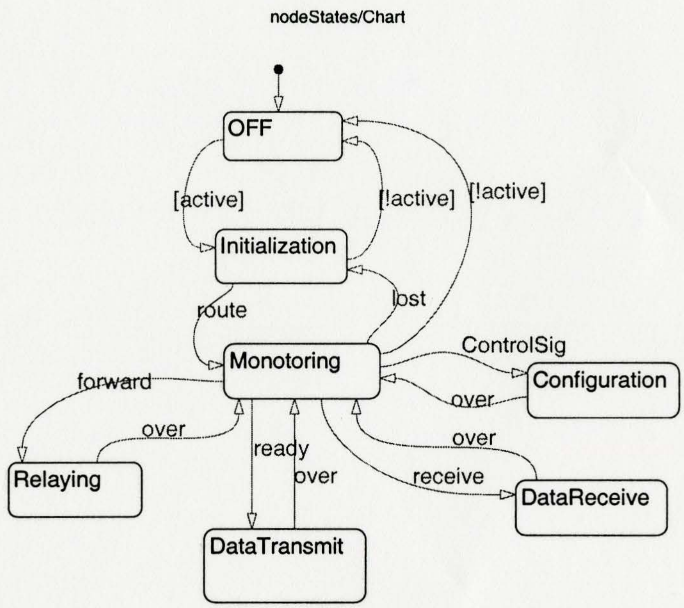

Figure 2.4: The states of CR node in mesh network

- The sponsor candidate is active and fully functioned in the mesh network.
- The sponsor candidate must be one of the nodes that the new node could find and has the shortest hops to the mesh BS.
- If two sponsor candidates have the same number of hops to their closest mesh BSs, then the candidate node selects the one with higher signal-to-noise-ratio (SNR).

To find a node in a mesh network is benefited from network configuration packages. Network configuration package is another basic signalling in a mesh network. Finding a node in a network is handled by a routing algorithm. In our mesh network simulation, the routing algorithm uses the zero-routing protocol. Each node needs to maintain a copy of the status of its current state, its neighbor states, the hop numbers, transmission powers, and their transmission schedules. The information is exchanged through mesh-network-configuration (MSH-NCFG) package. In our mesh network experiment, the information structure of a node about its neighbors is shown in the Table 2.1.

Item	Description
neighbors (Nbr)	List node IDs of the neighbors
Activity	b1: active, b2: transmit, b5: entry
Hops	0: backhaul, increase 1 for every additional hop
Current Tx Power	0: monitor. in 2dB steps, from 8dbm.
Maximum Tx power	the maximum transmit power for each Nbr
Next Tx slot	The symbol numbers from the current one
Next Tx length	The symbol numbers last

Table 2.1: Network status stored in each node

If a new node has a connection to backhaul network, it will be active at once and begin to enter the network configuration signalling session as a role of a mesh BS. Otherwise, the new node is called a candidate node and needs to synchronize with the network and goes through a sponsor procedure. While monitoring MSH-NCFG signals and analyzing their contents, the new node is able to find the network entry slot for network access. A network entry slot is the first slot in a network control subframe. And the network configuration information occupies coordinately the network configuration slots. A network configuration subframe is transmitted in the control channel periodically, while the other control subframes are for network scheduling control subframes, including central scheduling and distributed scheduling.
The sponsor procedure is detailed in Figures 2.5 and 2.6.

First, the candidate node needs to find a potential sponsor node to support its network access. When a candidate node is enabled, it keeps silent on its transmitter side

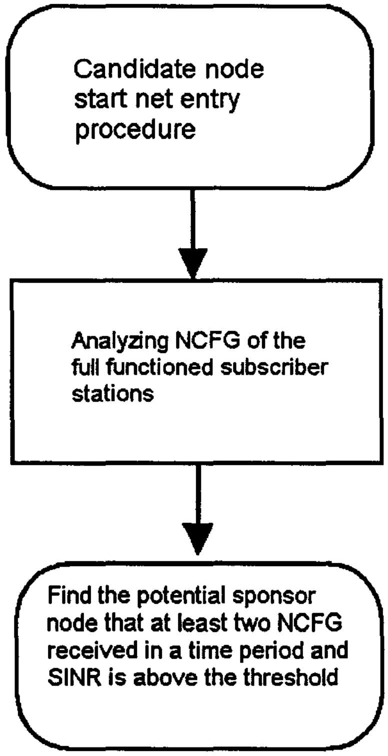

Figure 2.5: Procedure of network access

and begin to synchronize with the control channel. Then it analyzes control signals and estimates the signal qualities from those active nodes. At least two MSH-NCFG packages from a given node are received by the candidate node with an acceptable SNR level, then this node is selected as the potential candidate sponsor. The candidate node will launch the sponsor procedure shown in Figure 2.7. The mesh network entry package is transmitted in the network entry period in frames. The network entry package is transmitted in a random, contention-based fashion. Once the new node acquires the node ID, it can proceed to establish links to its neighbors other than the sponsor node. Limited by network routing and control signalling exchanging procedures, links should be established based on a duplex communication mechanism.

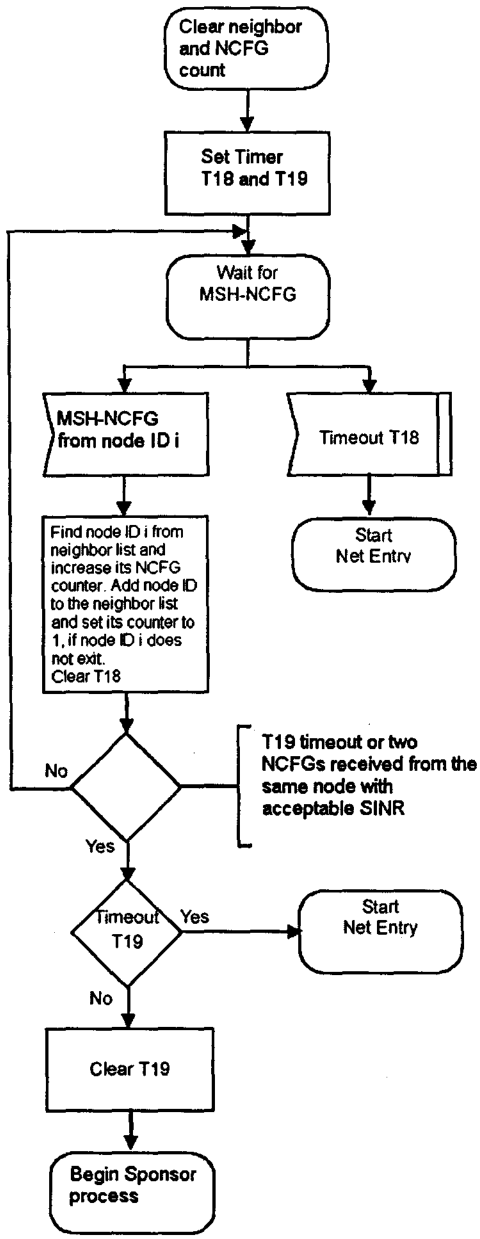

Figure 2.6: Procedure of finding the potential sponsor candidate

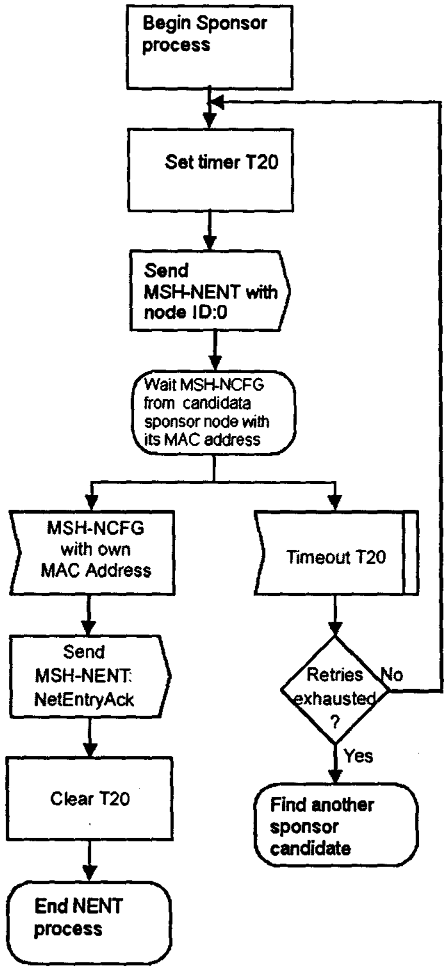

Figure 2.7: Procedure of sponsor process on candidate node side

The sponsor candidate may enter the sponsor procedure or reject if it is sponsoring another new node or the quality of the received signal is poor. The procedure of the sponsor process on a full functioned sponsor candidate side is shown in Figure 2.8.

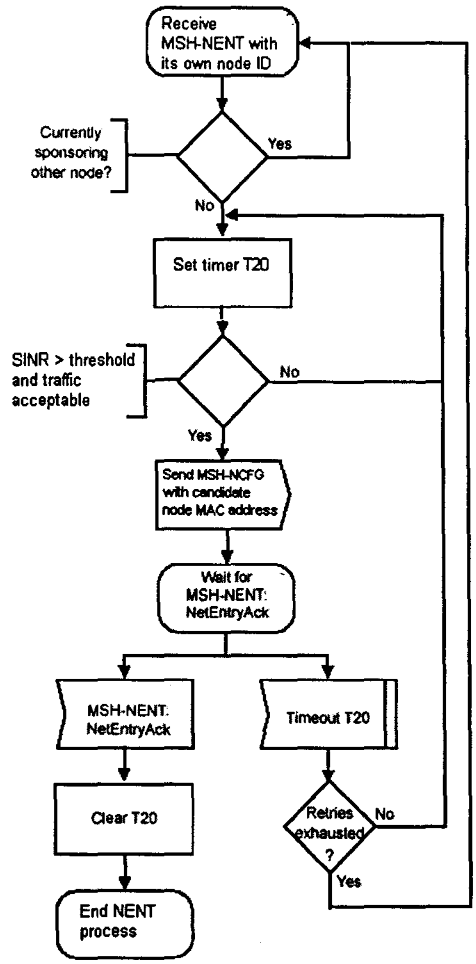

Figure 2.8: Procedure of sponsor process on sponsor candidate side

Once the sponsor procedure passes, the candidate node begins to transmit network scheduling and network configuration signals cooperatively within its extended neighborhood. In our mesh network experiment, the software flowchart is shown in Figures 2.6, 2.7, and 2.8. In the experiments, nodes are enabled and disabled randomly and the network control channel is verified to work properly for the network status update. The network signalling is an important part to make sure that the mesh network works.

The nodes operate on a pipeline and semaphore mechanism. The MAC layer and PHY layer exchange information on a pipeline, once the transmit pipeline is filled by the MAC layer, PHY layer will turn on its radio and begin to transmit that data. From the MAC layer point of view, if there are no data from the upper layer, nodes will only send their control signallings on schedule. The MAC signalling is transmitted frame by frame in Figure 2.9. There are two kinds of frames as shown in Figure 2.10. Frames will be allocated to symbols in the physical layer and transmitted on line.

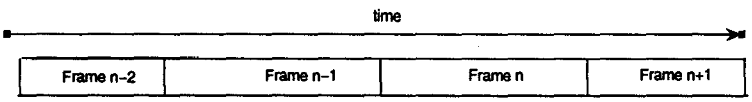

Figure 2.9: MAC frames in mesh network

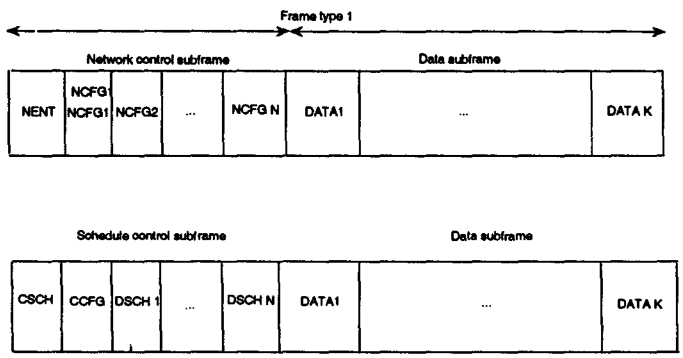

Figure 2.10: MAC frames details in mesh network

The PHY layer keeps on monitoring the transmit pipeline for the ready signals. Once the data are prepared by MAC in the pipeline, the PHY layer will send it according to a predefined mechanism. The data are divided into two catalogs: control data, and application data. The control data will go through control channels, while the application data go through traffic channels.

When a node needs to transmit data, it needs to exchange the scheduling information among its extended neighborhood. This procedure is realized using mesh-distributed-scheduling (MSH-DSCH) signals as shown in Figure 2.10. It experiences three steps: request period, grant period, and grant confirmation period. In the MSH-DSCH period, the parameters of channel allocation and transmit-power control are embedded in this information exchange.

Each node maintains two semaphores to exchange information between medium access control(MAC) layer and physical(PHY) layer. The MAC layer works at the frame level, while the PHY layer works at the symbol level.

The control channel is occupied in a cooperative way among extended neighborhoods. The control subframe and data subframe from each active node build up a frame in the MAC layer. Each active node has a transmit counter for the control channel. Each time the transmit counter of a full functioned node goes back to non-positive and there is no primary user occupies the control channel, the node will enable its transmit process to calculate the next transmit chance for control signalling. The length of MSH-NCFG is related to its active neighbor numbers, while the length of MSH-DSCH is related to its active connections to its own neighbours. They have variable lengths. MSH-NCFG consists of the node's information and neighbours' information, while MSH-DSCH consists of the link parameters. A node's next transmit opportunity of its control package is calculated, based on Figure 2.11.

In the software flowchart of the next transmit opportunity calculation, the mesh election is based on an algorithm in (IEEE802.16 2003).

2.2 Physical-Layer Implementation

The receive channel and the transmit channel are processed with ping-pong buffers.

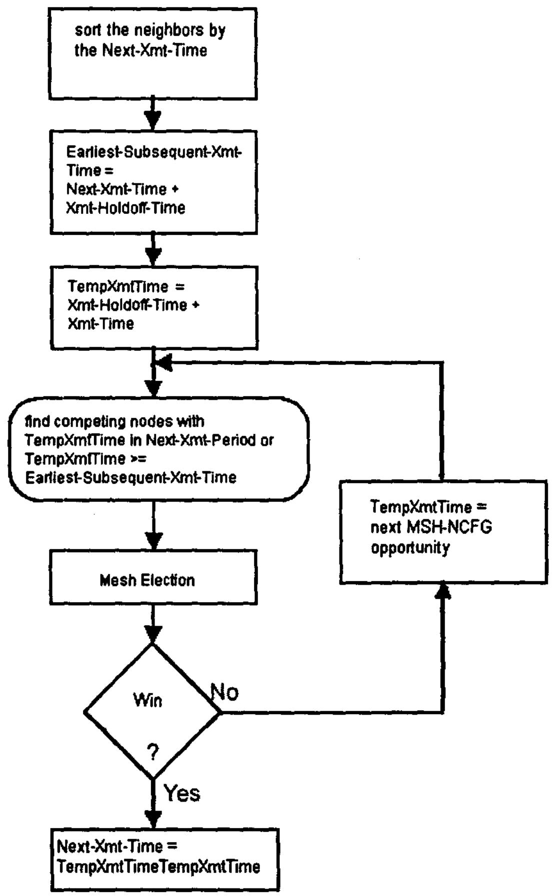

Figure 2.11: Procedure to determine Next-Xmt-Time

One buffer is for ongoing communication, transmit or receive; while another buffer is for processing. The nodes keep on monitoring their environment by processing the symbol based receive signals. Wireless HUMAN-OFDMA uses multi-tone modulation technology and is designed for NLOS operation in the 2-11GHz frequency bands. It is an amendment from 802.16 to be more suitable to a metropolitan environment. In 802.16a, there are two OFDM systems, OFDM and OFDMA. OFDM is introduced for less challenge applications; simply put, it is similar to a wireless local area network(WLAN) 802.11a. In OFDMA mode, on the other hand, the total available carriers are divided into subchannels and used for multiple accesses(IEEE802.16

2003).

A time-domain signal in OFDMA system is generated using inverse-Fourier-transformation (IFFT). In order to collect the multipath and maintain the orthogonality of the frequency bins, cyclic prefix is added in front of each symbol. An OFDMA symbol is made up of carriers, which determines the fast-Fourier-transformation (FFT) size. The carriers include data carriers, pilot carriers, and null carriers. The data carrier is for information-transferring, the pilot carrier is for channel-estimation, and the null carrier is for guard bands(Bingham 2000). In the OFDMA mode, the active carriers are divided into subsets of carriers. Each subset is named as a sub-channel. In the PMP network, a subchannel maybe intended for different receivers on the downlink, while on the uplink a transmitter maybe assigned to one or more subchannels, and several transmitters may transmit in parallel. The OFDMA transmission signal is defined as

$$s(t) = \sum_{i=1}^{K} \mathrm{Re}(e^{j2\pi f_c t} \sum_{k \in \mathbf{N}_i} c_k e^{j2\pi k \Delta f (t - T_g)}) \tag{2.1}$$

where t is the time, c_k is the complex data to be transmitted on the k^{th} frequency bin. It corresponds to a point in a quadrature amplitude modulation(QAM) constellation. T_g is the guard time. Δf is the frequency spacing. The $\mathbf{N}_i$ denotes tones belonging to node i. In OFDMA technology, the signal is defined in two dimensions: one dimension is the time domain, represented by the symbol series; the other dimension is the frequency domain, denoted by the tones as shown in Figure 2.12.

In a CR mesh network, the sub-carriers to be used by SS depend on the time-varying environment. Since a frequency offset exists among SSs, each SS should try to select its own sub-carriers as adjacent as possible. The pilot tones are arranged in each sub-channel.

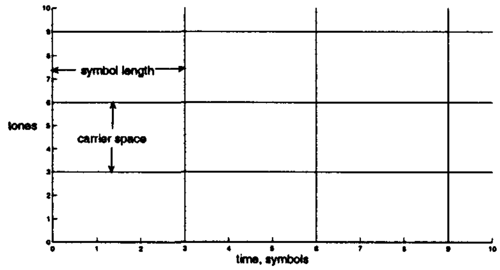

Figure 2.12: Data region of the OFDMA allocation

For OFDMA, $F_s = \frac{8}{7}BW$. In our experiment, we adopt the following configurations as used by Intel 802.16 scalable OFDMA system(Yaghoobi 2004) in Table 2.2.

Item	Value
System bandwidth (MHz)	20
Sampling frequency (Fs,MHz)	22.857
Sample time (1/Fs,nsec)	44
FFT size (NFFT)	2048
Subcarrier frequency spacing	11.16071429 kHz
Useful symbol time ($Tb = 1/\Delta$)	89.6 μs
Guard time (Tg=Tb/8)	11.2 μs
OFDMA symbol time (Ts=Tb+Tg)	100.8 μs

Table 2.2: Network status stored in each node

In the frequency band, carrier allocations are shown in Table 2.3.

In each subchannel, there are five pilot tones that we can use for DBTMA medium access protocol. In a data-traffic channel, the transmitter will use three pilot positions. The one pilot position with fixed position is used for channel quality estimation with a predefined pseudorandom sequence. The other four pilot positions change from one frame to another. The first two random positions are for RTS tones. Two other random positions are for receiver response with CTS tones. With this setting, the DMTMA is embedded in the physical layer naturally.

In the OFDMA system, the channel coding procedures include randomization, FEC

Parameter	Value
Number of DC carriers	1
N_{used}	1696
Guard carriers: left/right	176/175
$N_{subchannels}$	32
$N_{subcarriers}$	53
$N_{datacarriers}$ per subchannel	48

Table 2.3: OFDMA carrier allocation in CR mesh network

encoding, interleaving and modulation. The physical layer simulation of the wireless OFDMA baseband is shown in Figure 2.13. It is realized with MATLAB/Simulink models, with some modules implemented by S-function.

On the transmitter side, the source data are first randomized with a scrambler, which is shown in Figure 2.14. A scrambler is important for synchronization and DC suppression. Then the signal will go through a forward-error correction(FEC) encoder which is the concatenation of a block error code using Reed-Solomon codeword and a convolutional code with puncturing to improve coding efficiency. This Reed-Solomon code is derived from a shortened systematic RS (N=255, K=239) code, using GF(256) with the field generator polynomial is(IEEE802.16 2003)

$$p(x) = x^8 + x^4 + x^3 + x^2 + 1 \tag{2.2}$$

The Reed-Solomon codewords are interleaved to scatter low SNR information bits and improve burst error-correction capability(Haykin and Moher 2004). Each RS codeword is encoded by a binary convolutional encoder with the code rate of 1/2 and generator polynomials of $[171, 133]_{OCT}$. Detailed description of the encoder is shown in Figure 2.15. The coded signal is mapped on to quadrature amplitude modulation(QAM) symbols on each data subcarrier, with binary phase-shift keying, quaternary phase-shift keying(QPSK), 16-QAM, and 64-QAM modulation techniques,

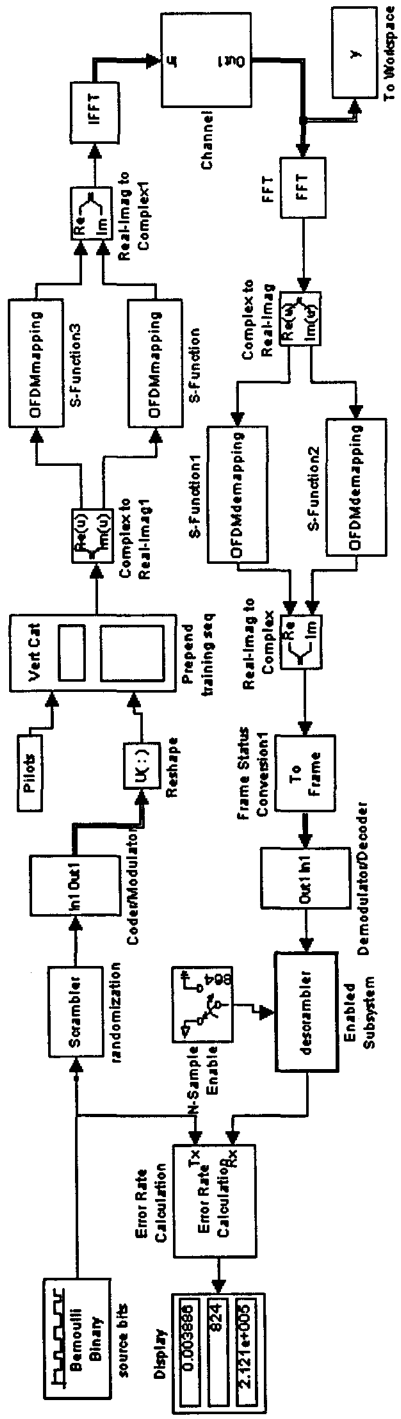

Figure 2.13: Physical layer loopback of OFDMA implementation

as shown in Figure 2.18. This is the baseband process. The in-phase and quadrature components of the baseband signal then go through quadrature modulator supplied with a carrier frequency of 2 - 11GHz.

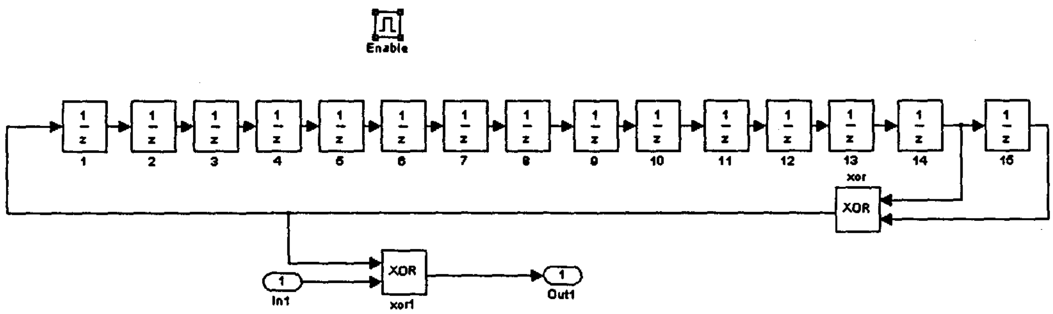

Figure 2.14: Scrambler of the physical layer

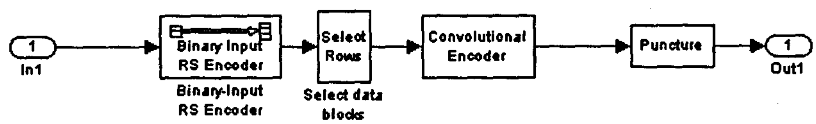

Figure 2.15: FEC blocks

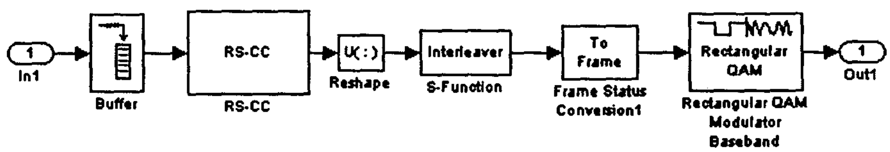

Figure 2.16: Encoder of the physical layer

Detailed description of the receiver path of demodulation and FEC decoder is shown in Figure 2.17.

These Simulink subsystems shown in Figures 2.15, 2.16, and 2.17 are integrated into the Simulink model in Figure 2.13. The simulation result can be monitored

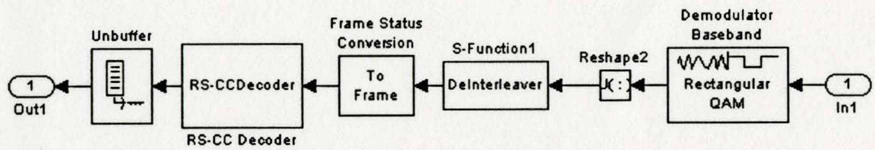

Figure 2.17: Decoder of the physical layer

through the 'display' block. Figure 2.13 shows the simulation result with BER of $3.9e-3$. Figure 2.18 shows the model running result of the receive signal scatter with Additive White Gaussian Noise(AWGN) only.

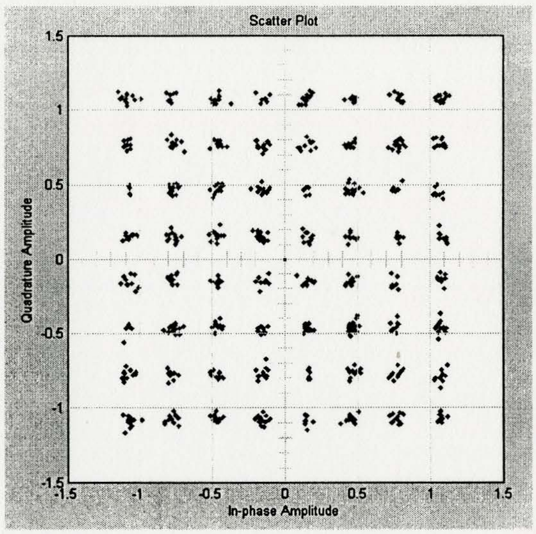

Figure 2.18: Scatter signal in OFDMA with AWGN only

Subcarriers are functioned as guard subcarriers, pilot subcarriers, and data subcarriers. The pilot carriers are for handshake and channel state-estimation. The pilot carriers send the dual-busy tone and the pseudorandom sequence. The guard carriers are set to zero so that the out-of-band signal power spectrum density(PSD) rolls off under the interference temperature mask(Haykin 2005). Interference temperature is used to measure the interference level in cognitive radio. It is a regulation parameter determined by policies from organizations like FCC. Each link in the CR mesh network only occupies a part of the total available bandwidth. Some adjacent subcarriers are grouped into sunchannels, so that links can work on a subchannel basis to reduce the inter-carrier-interference (ICI). Figure 2.19 shows the transmit signal of a 2048 subcarrier case, with 256 subcarrier grouped to a subchannel.

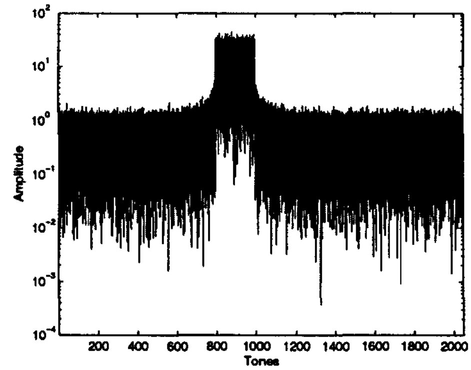

Figure 2.19: One link spectrum with clear background with AWGN only

Summary

In this chapter, we described the realization of MAC layer signalling and physical layer processing in CR mesh network. In a MAC layer, the exchange procedure of control signals are described in detail. Nodes in a mesh network use these signalling to exchange information. The MAC signalling prepares a logical path for dynamic channel allocation and transmit-power control introduced in latter chapters. The MAC layer information from one node must go through physical layer so that other nodes can acquire it. The physical layer realization uses Simulink; it simulates the processing of a transmit path and a receive path. The blocks include randomization, concatenated Reed-Solomon and convolutional channel coding, puncture, tone mapping, and modulation subsystems. The physical layer realization provides a physical path for connections among nodes in the CR mesh network. The Simulink model can be easily ported to current digital signal processing and micro-controller chips for hardware realization if so desired.

Chapter 3

Dynamic-Frequency Selection

Multiple-access techniques in current cellular systems are classified into three categories or combination thereof: frequency-division-multiple-access, time-division-multiple-access, and code-division-multiple-access. In these networks, the system performance regarding power control, access control, and channel allocation techniques have been widely researched(Shepard 1995). However, most of the research effort has focused on one single system problem only. Wireless resources allocated to that system are shared by users belong to that system only. In recent years, some work has been done regarding seamless handovers among heterogeneous networks(Floroiu, R., Sisalem, and Voglimacci 2003)(Cuomo, Martello, and A.Baiocchi 2002), such as between cellular and WLAN networks. Sharing wireless resources among different systems such as WLAN and radar systems in Europe on 5GHz frequency band makes dynamic frequency selection (DFS) a mandatory. The essence of introducing CR is to improve spectrum efficiency. So the requirement of co-existing with primary users makes DFS a mandatory feature in CR users. To co-exist with primary users, who were already assigned to work in those bands, CR has to be very agile within the ambient wireless environment.

In the context of a OFDMA-based CR system, the problem of DFS becomes a dynamic sub-channel selection problem. A DFS problem is different but has many similarities with a dynamic channel allocation (DCA) problem. The goal of a DCA algorithm is to increase the channel capacity by reducing co-channel interference and inter-channel interference. The goal of a DFS problem in CR networks is to reduce collisions between CR users and primary users. In a CR system, the DCA algorithm is realized by the cooperation among CR users; while the DFS algorithm is realized by every CR to avoid competition with primary users. In the thesis, we focus on the DFS algorithm in a CR system so that CR users could co-exist with primary users. Although in IEEE 802.11 and IEEE802.16 standard series, there are DFS requirements to guarantee their co-existence with radar systems, DFS algorithm is not defined. In (Medidi and Daptardar 2004), a DFS algorithm is presented, based on the receive signal strength before transmission and signal quality detection during transmission. In (McFarland and Green 2003), a DFS algorithm is used in WLAN systems by swapping channels through cooperation among access points.

Like using a zero-routing protocol in a MAC layer of a mesh network, here we introduced a DFS algorithm that is suitable for CR mesh networks. It includes two basic methods of channel allocation: measurement-based method, and status-based method. When using the measurement-based method, a CR node needs to scan each channel periodically to find spectrum holes. A spectrum hole is defined in (Haykin 2005) as "a band of frequencies assigned to a primary user, but, at a particular time and specific geographic location, the band is not being utilized by that user." In the status-based method, each node acquires the channel status of busy/idle through monitoring the exchanges of the MAC-layer control packets. With channel usage information, CR nodes are able to select vacant channels for their own linkages. We adopt a combination of the two methods in the CR mesh network for channel assignment. The spectrum holes are found through measurement, and the busy status of the channel is based on signalling. The channels to be assigned should be in accord with both results. *This hybrid channel allocation method makes it possible for CR systems to avoid both collisions with primary users and collisions with other CRs because of weak receive signals.*

In the single-channel cases discussed in (Li, Haas, Sheng, and Chen 2003), the MAC-layer protocol cannot process both the traffic channel and control channel at the same time. However, in multi-channel cases using OFDMA mode, a node in the mesh network can monitor the control channel and process the traffic channels at the same time. This is the benefit of using the multi-carrier modulation method.

3.1 Dynamic Frequency-Selection in a CR Mesh Network

In CR products, DFS algorithm is important to protect the primary users and to improve spectrum utilization. DFS is the basis of the coexistence of primary users and CR users. If CR causes severe interference to primary users, it may be kicked out of operation. The wireless environment analysis of a CR user termed as "radio scene analysis" could provide the instantaneous usage of the frequency band(Haykin 2005). However, when a CR wants to transmit something, it should be confident enough that not only the frequency band is available at the time that it begins to transmit, but also that during its transmission the primary user may not come back to interrupt the data transmission of the CR, and in turn be polluted by the CR. Channels are allocated before data transmission takes place. Since the data transmission happens in the coming time period, the CR needs to predict the possible frequency usage in its transmission period. The prediction is based on history information of the wireless environment. By continually monitoring channel activity of the wireless environment, the CR's knowledge database about its environment is established. The optimal spectrum holes are those channels that satisfy CR link requirement and have a higher probability of being vacant during CR transmission.

In the CR system, we propose a DFS algorithm that utilizes the distribution of traffic load in each frequency band. This DFS algorithm has the following characteristics:

1. Scanning the frequency spectrum to find spectrum holes.
2. Analyzing the spectrum usage to find the primary users.
3. Analyzing the primary users' traffic statistics.
4. Predicting the spectrum usage pattern in its coming data transmission period.

Our DFS algorithm of CR users could effectively avoid collisions with primary users. It is based on two strategies:

1. Avoiding the frequency band that is used by primary users
2. Reducing the interference that it introduces into the environment.

Since the primary user's traffic statistics are an important factor in the CR DFS algorithm, availability of traffic statistics for the primary user may greatly reduce the chance of co-channel interference between the CR and the primary user. Primary users may use circuit-switching or packet-switching mechanisms. Circuit-switching is usually modeled as a Poisson process, while the packet-switching traffic varies with the information type. It is usually simulated with uniformly distributed blocks within the accepted packet size limit and the minimum packet length(Mills 1983).

Our CR DFS algorithm can be also adjusted to suit a circuit-switching system or large packet-size packet-switching system, if so required. We suggest that before a link is established, mesh BS and SSs must first of all make sure the channels they select are not occupied by the primary users. Also during the communication phase, they must switch channels to some low-collision probability channels after transmit on the allocated channels for a while. The switching time is decided by the traffic patterns of primary users that occupy those channels.

Different primary users have different traffic patterns. There are two main classes of traffic patterns, which are deterministic pattern and random pattern. For the deterministic pattern, the radios of the primary users may turn on or off for a very long time. These kinds of primary users may be TV or AM/FM broadcast radios. Most communication systems, however, have a random traffic pattern, the cellular system being one good example.

3.1.1 Deterministic pattern

A primary user with deterministic traffic pattern has a fixed transmission time. If its traffic pattern is available to CR during the primary user OFF period, the CR can use its frequency band. In this kind of traffic pattern, the probability of the CR successfully occupying these bands is fully understood. It is either totally sure of availability or the impossibility of using these bands at all.

3.1.2 Random pattern

In the random pattern case, dynamic frequency selection (DFS) can only select the frequency bands with a high probability of vacancy during CR transmission. The data arrival in some wireless frequency bands can be modeled as a Poisson process as in a public switched telephone network. For a Poisson process, let $p_n(t)$ be the probability of n arrivals in a time interval of length t, for $n \geq 0$; then

$$p_n(t) = \frac{(\lambda t)^n}{n!} e^{-\lambda t} \tag{3.1}$$

If the arrival rate λ is available, then the probability of the primary user being free in the CR transmit period is available. For a circuit-switched system, the service time, related to the ON status, is usually modeled as an exponential distribution with the service rate μ. For a packet-switched system, the service process can be modeled as uniformly distributed within the $[t_{\min}, t_{\max}]$ time period, which corresponds to the minimum packet size and the packet size limit, respectively:

$$p_n(t) = \frac{T_s}{t_{\max} - t_{\min}} t \tag{3.2}$$

where T_s is the sampling period.

In a real-life wireless system, the traffic process of a single user is not autonomous but subject to flow control at the end hosts and congestion control at routers. So the traffic patterns also depend on congestion and receive windows. Much of the literature regarding traffic models has discussed cases when the Poisson model is not accurate for real traffic, such as local area networks(Cooper, Zeidler, and Bitmead 2004). Natural traffic also shows long-range dependencies since congestion is more frequent. But this characteristic is not been covered in the Poisson traffic model.

All of the random traffic patterns are time dependent. The CR user should establish a knowledge database about its environment through continuously tracking the traffic pattern of the spectrum it concerns. The probability of the primary user being free is a very important parameter in CR DFS algorithm.

3.2 Traffic Analysis

The traffic pattern of the primary user varies with time, frequency, and space. To characterize the traffic pattern, a generic model is required. Here the Gaussian Mixture Model (GMM) is selected for this purpose.

GMM is a very generic model, which can be used to model any probability distribution, given an adequate number of kernels. For the traffic pattern analysis, the probability density function (PDF) of a one dimensional GMM is defined by(Mclachlan and Basford 1992):

$$p(x) = \frac{1}{\sqrt{2\pi}} \sum_{k=1}^{K} \frac{w_k}{\sigma_k} \exp^{-\frac{(x-\mu_k)^2}{2\sigma_k^2}} \tag{3.3}$$

and its Cumulative Distribution Function (CDF) is

$$F(x) = \sum_{k=1}^{K} \frac{w_k}{2}(1 + erf(\frac{x - \mu_k}{\sigma_k \sqrt{2}})) \tag{3.4}$$

where w_k, μ_k, and σ_k are the mixing weight, expectation and covariance of the k^{th} Gaussian kernel respectively. K is the total number of Gaussian kernels. These $3 * K$ parameters need to be estimated through observations of the primary user's traffic usage. But since the environment is slowly time varying, the estimation must converge at a fast rate compared to the variation of the environment and be able to track traffic pattern changes of primary users.

3.2.1 Parameter estimation of GMM with EM algorithm

There are K Gaussian kernels in this GMM model. Instead of finding the best **k** given an estimation of parameters at each iteration, we just need to compute a distribution over the K kernels without knowing from which mixture each sample was drawn. Also the operation of primary users in that environment is unavailable to CR users. It is an unobservable variables in CR DFS. Here the Expectation Maximization(EM)(Mclachlan and Basford 1992) algorithm is used to evaluate the parameters. The EM algorithm provides a recursive solution to find the maximum likelihood estimation of the problem. The log-likelihood function for the observation data set $\mathbf{x} = x_1, x_2, \cdots, x_N$ is given by

$$L(\lambda) = \log(p(\mathbf{x}|\lambda)) \tag{3.5}$$

where λ is a set of parameters to be estimated.

The nice feature of the EM algorithm is that the likelihood for the data specification can never decrease in an EM sequence. Hence, the log likelihood under the mixture model satisfies the condition

$$L(\lambda^{(i+1)}) \geq L(\lambda^{(i)}) \tag{3.6}$$

that is

$$\lambda^{(i+1)} = \arg\max_{\lambda^{(i)}} \sum_{\mathbf{x}} \sum_{\mathbf{y}} P_{\lambda^{(i)}}(\mathbf{y}|\mathbf{x}) \log P_{\lambda^{(i)}}(\mathbf{y}, \mathbf{x}) \tag{3.7}$$

where $\mathbf{y}$ denotes the incomplete observations.

Baum-Welch or forward-backward algorithm is a special case of the EM algorithm. Let $\alpha_k(i)$ be the probability of the partial observation sequence $O_{1:k} = [o_1, o_2, \cdots, o_k]$ to be produced by all possible state sequences that end at i^{th} state $q_k = i$; then the probability of the partial observation sequence is the sum of $\alpha_k(i)$ over all N states

$$\alpha_k(i) = P(o_1, o_2, \cdots, o_k, q_k = i|\lambda) \tag{3.8}$$

where λ is the parameter set. Then the probability of an observation sequence given the parameters is

$$P(o_1, o_2, \cdots, o_k|\lambda) = \sum_{i=1}^{N} \alpha_k(i) \tag{3.9}$$

First, in the forward algorithm, the probabilities for the single-symbol sequence are calculated as a product of initial j^{th} state probability π_j; and the emission probability $e_j(o_1)$ of the given symbol o_1 in j^{th} state is defined by

$$\alpha_1(j) = \pi_j e_j(o_1), \quad j = 1, 2, \cdots, N \tag{3.10}$$

Then the recursive formula

$$\alpha_{k+1}(j) = [\sum_{i=1}^{N} \alpha_k(i) a_{ij}] e_j(o_{k+1}), \quad j = 1, 2, \cdots, N; k = 1, 2 \cdots, L-1 \tag{3.11}$$

is applied. a_{ij} denotes the state transition probability. Finally the probability

$$P(o_1, o_2, \cdots, o_L|\lambda) = \sum_{i=1}^{N} \alpha_L(i) \tag{3.12}$$

is computed.

Let $\beta_k(i)$ be the conditional probability of the partial observation sequence from o_{k+1} to the end $O_{1:k} = [o_{k+1}, o_{k+2}, \cdots, o_L]$. It is produced by all state sequences that start at i^{th} state $q_k = i$. Then the probability of the partial observation sequence is the sum of $\beta_k(i)$ over all N states

$$\beta_k(i) = P(o_{k+1}, o_{k+2}, \cdots, o_L|q_k = i, \lambda) \tag{3.13}$$

where λ is a controllable parameter. Then

$$P(o_1, o_2, \cdots, o_k|\lambda) = \sum_{i=1}^{N} \pi_i e_i(o_{k+1})\beta_k(i) \tag{3.14}$$

Similarly, initialization of the backward algorithm is defined by

$$\beta_L(j) = 1, \quad j = 1, 2, \cdots, N \tag{3.15}$$

and the backward recursion is

$$\beta_k(j) = [\sum_{i=1}^{N} \beta_{k+1}(i) a_{ji} e_i(o_{k+1})], \quad j = 1, 2, \cdots, N; k = L-1, L-2 \cdots, 1 \tag{3.16}$$

Finally, we have

$$P(o_1, o_2, \cdots, o_L|\lambda) = \sum_{i=1}^{N} \pi_i e_i(O_1)\beta_1(i) \tag{3.17}$$

The forward-backward algorithm uses the probabilities of transitions and emissions to approximate the corresponding counters. The recursion includes

$$A_{ij} = \frac{1}{P(O|\lambda)} \sum_{i=1}^{L-1} \alpha_i(l) a_{ij} e_j(O_{l+1}) \beta_j(l+1) \tag{3.18}$$

$$E_i(k) = \frac{1}{P(O|\lambda)} \sum_{l:o_l=k} \alpha_i(l)\beta_i(l) \tag{3.19}$$

where a_{ij} and $e_i(k)$ are the normalized value of A_{ij} and $E_i(k)$, respectively(Petrushin 2000).

A moving time-window is applied for tracking the slowly varying environment. In the arrival-pattern analysis, the observations are the intervals of the adjacent transmit start times. In the service-pattern analysis, the observations are the duration of transmit periods. And in the spectrum-hole analysis, the observations are the channel free periods. The observations include two parts: arrival time, and service time as shown in Figure 3.1.

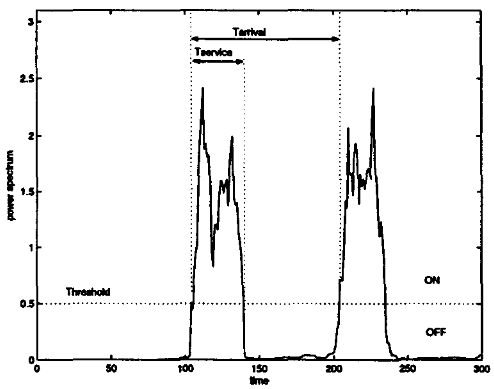

Figure 3.1: Spectrum analysis.

A primary user's traffic probability density function is approximated by GMM. There are possibly some humps in the PDF that can be represented by Gaussian kernels. Training the Gaussian model corresponds to classify observation data points to Gaussian kernels. The parameters of Gaussian mixture are learned by the Forward-backward algorithm which includes two phases: initialization and learning. In the initialization period, we use the K-means clustering algorithm(Resch 2004) to set initial parameter values. It classifies a data set into K groups of Gaussian distributed subsets which can be described in the following steps:

1. Select K different data points randomly from N data points, and set the K points as the centers. If $N < K$, then K is reduced to be less than or equal to the number of different points.

2. Cluster the N data points to the K groups, based on the minimum-distance criterion.

3. In each group, find the new center. Go back to the previous step, until convergence is reached.

4. Set the mean and variance of each group based on the clustering result, and set the mixture weights randomly where they are all positive and sum to one. $\sum_{k=1}^{K} w_k = 1$

In the learning period, the forward-backward algorithm is able to find a new sequence of parameters over the previous one with a higher log likelihood in each iteration, so that it increases the probability of the overall observations. The parameters of the GMM are updated in each iteration. The mixture weights are updated first, then the means and variances are updated corresponding to the mixture weights(Resch 2004). The learning period includes the following steps:

1. Calculate the probabilities of the mixture and the individual Gaussian kernel for each observation D_t, which are denoted as B_t and $B2_{k,t}$.

2. Use the forward and backward methods introduced above to calculate α_t and β_t, then update the individual Gaussian kernel probabilities $\gamma_t = \alpha_t \beta_t$. And the new individual Gaussian kernel probabilities $\gamma_{k,t}$ are updated according to

$\gamma 2_{k,t} = \frac{B2_{k,t}}{B_t} w_k \gamma_t$. If B_t equals zero, the new individual factor probabilities are set to zero.

3. Calculate the new mixture weights. $w'_k = \sum_t \gamma 2_{k,t}$

4. Calculate the average value. $\bar{D}_k = \sum_t \gamma 2_{k,t} D_t$

5. Calculate the square average, $\bar{D^2}_k = \sum_t \gamma 2_{k,t} D_t D_t$

6. Normalize the mixture weight with $w_k = \frac{w'_k}{\sum_k w'_k}$

7. Update the mean $\mu_k = \frac{\bar{D}_k}{w'_k}$

8. Update the variance $\sigma_k^2 = \frac{\bar{D^2}_k}{w'_k} - \mu_k^2$.

9. calculate the log-likelihood. $\sum_t \log \alpha_t$

When the difference between two consecutive values of log-likelihood function is less than a threshold; or when the maximal number of iterations is exceeded, the iteration stops. The GMM can be used to model different kinds of traffic models. In Figure 3.2, the traffic is uniformly distributed, which is a characteristic of packet-switched systems without congestion. There are 3000 point observations and they are randomly allocated in a range of $[-20, 40]$. The EM learning algorithm converges after 10 iterations with 8 Gaussian kernels, which is a good example.

Figure 3.3 applies to a Poisson process, which describes the arrival sequence of circuit switched systems. There are 1000 point observations, and the arrival rate of Poisson process is set to $\lambda = 6$. The EM learning algorithm converges after 8 iterations with 8 Gaussian kernels.

Figure 3.4 shows the EM learning performance result for a complicated distribution. There are 3500 point observations, in which 1000 points came from a Poisson distribution with $\lambda = 6$; 500 points came from another Poisson distribution with

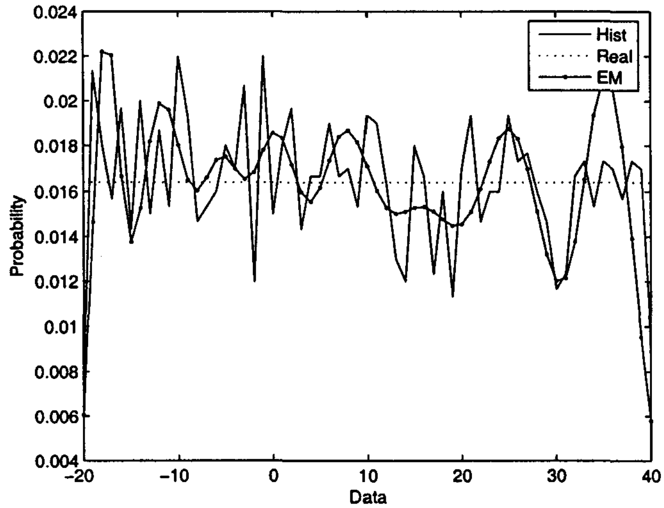

Figure 3.2: The EM learning result for the uniformly distributed traffic scenario

$\lambda = 17$; and another 2000 points came from a Gaussian distribution with $\mu = 10$ and $\sigma = 10$. This time, the EM algorithm converges after 12 iterations with 8 Gaussian kernels to estimate the mixed probability distribution of two Poisson distributions and a Gaussian distribution.

The results shown in Figures 3.2, 3.3, and 3.4 are testimony to GMM's versatility.

3.2.2 Simulation result of the dynamic channel allocation in WLAN

In WLAN, the MAC layer protocol adopts the Carrier-sense-multi-access/collision avoidance(CSMA/CA) mechanism. Since in a wireless network, the node cannot detect a channel if it transmits at the same time in the same channel, the collision cannot be detected as that in the Ethernet. The CSMA/CA protocol is shown in Figure. 3.5

It can be illustrated in the steps shown in Table 3.1.

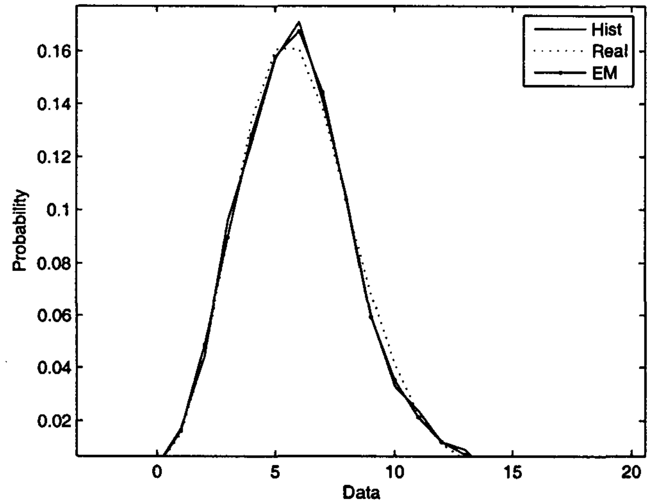

Figure 3.3: The EM learning result for the Poisson traffic scenario

Our simulation is based on Poisson arrival, uniformly distributed service time with the CSMA/CA MAC layer protocol. The time occupied by different packets is normalized according to the longest service time. We suppose the service time of the combination of data and END packets are uniformly distributed in $\frac{0.4}{\lambda}[1/4, 7/4]$. Waiting period for collision detection is uniformly distributed in $\frac{1}{\lambda}[0, 0.1]$ and $\frac{1}{\lambda}[0, 1]$, where the parameter λ represents the arrival rate. The normalized channel available and occupied histograms are shown in Figure 3.6 and Figure 3.7, respectively.

Using the EM algorithm to learn the channel availability probability shows a very good match to the GMM with histograms. We conclude that the GMM can be used by CR DFS algorithm so that CR could coexist with other systems in use.

3.3 DFS of CR System Based on Traffic Analysis

CRs can work in two ways:

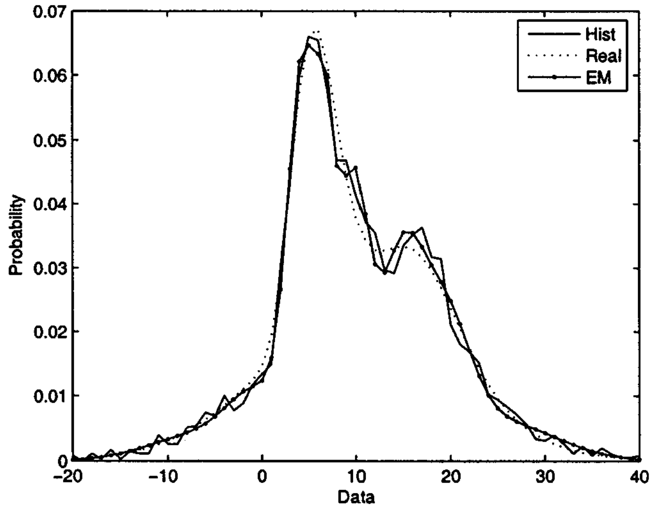

Figure 3.4: The EM learning result for the irregular traffic scenario

1. A CR can operate on a not-to-interfere basis. It senses the RF energy in a particular band, at a particular time and in a particular place. If it finds that the power in a particular slot is less than the interference level defined by the interference temperature, it can operate on that band with a distinctive power level by using the OFDMA method.

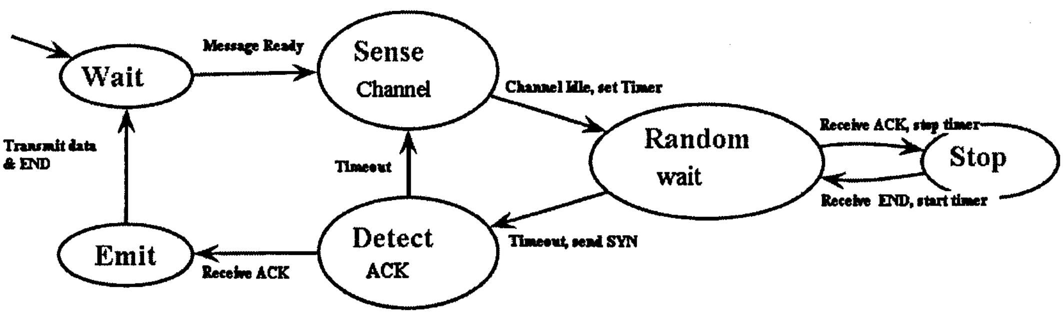

Figure 3.5: The MAC protocol of CSMA/CA

	User 1			User 2			User 3			
Step	state	trans	recev	state	trans	recev	state	trans	recev	event
1	wait			wait			wait			
2	sense			wait			wait			data1
3	Random			wait			wait			
4	Random			sense			wait			data2
5	Random			Random			wait			
6	Random		SYN	Random	SYN		wait		SYN	Timeout2
7	Random			Detect			wait			
8	Random		ACK	Detect		ACK	wait	ACK		
9	Stop		Data	EMIT	Data		wait		Data	
10	Stop		END	EMIT	END		wait		END	
11	Random			wait			wait			

Table 3.1: CSMA/CA protocol stateflow

2. A CR can also operate below some pre-determined acceptable interference temperature, such as using ultra wide band(UWB) or CDMA modes. This concept is addressed in the Spectrum Policy Task Force report (FCC 2002).

In this thesis, CR works on a not-to-interfere basis, that is the first work mode. We select the availability of the channel as the main factor of DFS. Other factors (e.g. channel estimation) decide the transmission method and the burst duration, and also further influence the DFS algorithm.

Our experiments use the following cases to illustrate that the traffic model based DFS can greatly increase the system capacity and decrease the cost of the packet communication. The parameters we select in our comparison with receive signal strength (RSS) based DFS include the average delay of packets and the average power consumed by a packet unit. The simulation results show that the exploitation of CR users is not only harmful to primary users, but also to themselves. There are two scenarios of the relationship of CR users and primary users:

1. The impact is from primary users to CR users, but not vice verse. In this case, we

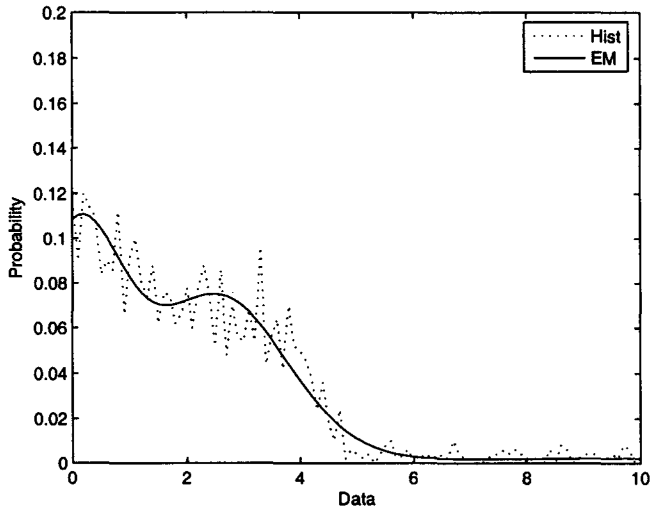

Figure 3.6: The channel free probability of M/G/1 model with small wait collision period CSMA/CA

do not consider the issue of penalties. That means the primary user is not affected by CR users. However the primary user may cause a CR user to be unable to work. We will illustrate that even in this case, a DFS algorithm based on RSS performs worse than an CR system with DFS based on RSS and traffic models.

2. In the second scenario, collisions between CR users and primary users has mutual impacts. In this case, primary users add a penalty to the CR users if collision happens. The penalty rate can further control CR users' behavior of their greedy characteristic.

3.3.1 Simulation platform setting

We set up a virtual wireless environment for our experiment, which is used to illustrate the benefit of our DFS algorithm. The DFS reduces the collision probability of CR user with primary users so that the throughput of both primary users and CR users themselves are improved. In CR radio scene analysis, the RF real signal is demodulated to the baseband complex signal for analysis. Since the wireless en-

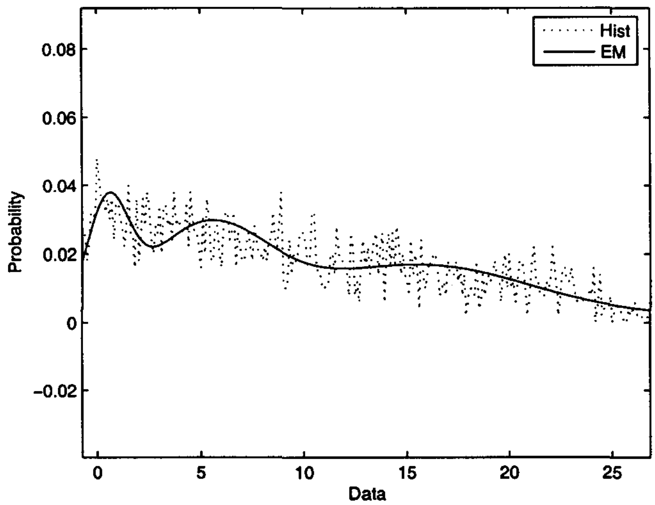

Figure 3.7: The channel free probability of M/G/1 model with large wait collision period CSMA/CA

vironment is time varying, a moving time domain window with overlap is used for radio scene analysis. Suppose the window length equals to N_{window}, and the moving step is N_{move}. The N_{window} samples, denoted by Dt, will pass through a multitapper spectrum analyzer to get a snap shot of the environment(Haykin 2005). Multi-tapper spectrum analyzer is introduced in (Haykin 2005) to be an effective way in radio scene analysis to estimate the interference level. These successive and slow varying observations are the preprocessed data in a frequency domain Df. This procedure is shown in Figure.3.8

Here, the delay line length is N_{window}, the zero-hold sampling period is f_s/N_{move}, and the spectrum analyzer is based on a multitapper spectrum analysis method.
At the very beginning, the CR system has no knowledge about the primary users in the environment around it. Only by learning could it work in this environment, and that is the big advantage of CR. With those snapshots, the first step of analysis will be segmentation and grouping of the frequency band to the primary users.

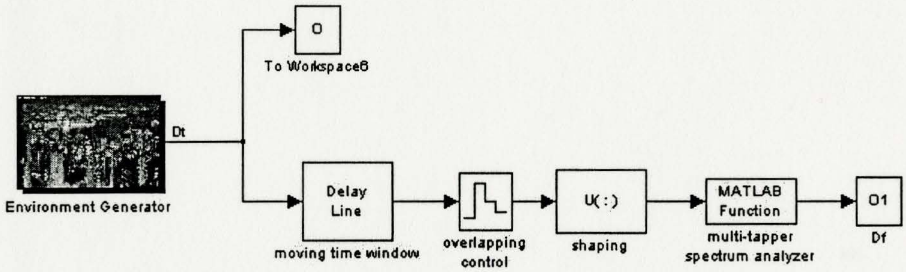

Figure 3.8: Spectrum analysis.

The grouping and segmentation will reduce the traffic tracking complexity, since the whole band belonging to a primary user can be treated as one object. Otherwise, the frequency bands have to be analyzed using the same frequency bandwidth as the analysis resolution with high computational complexity.

Here we adopt a proximity method to group those bands with high correlation coefficients of power changing status. In order to eliminate the border effect, the grouping method keeps on calculating the correlation coefficients between the group center and the interested band. The center moves as new bands are added in.

After grouping, the primary user's on-off pattern in each group is extracted for traffic analysis and tracking using EM algorithm. Since the transmit power in each band is different, we cannot use a fixed threshold for all bands. The relative power changing in two sliding windows is extracted here for the primary users' on/off status detection. The length of the two sliding windows is different. As the windows move, if the transmit status of the primary user changes, the average powers per sample of the two windows show distinctive difference. When the difference of the average power per sample exceeds a threshold, it means that the transmit status of primary user is switched. In our simulation, the environment generator is shown in Figure.3.9.

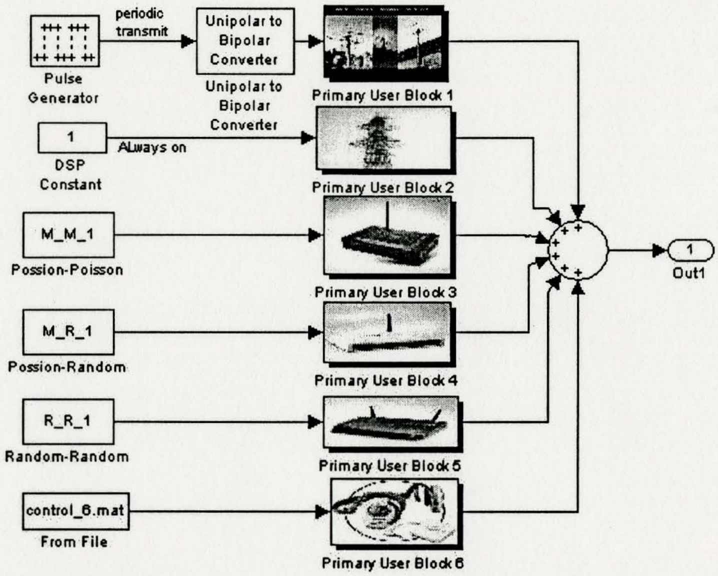

Figure 3.9: The wireless background generator.

In this virtual wireless environment, each primary user block is configured by its traffic pattern, center frequency, bandwidth and transmit power. The details of the primary user block are shown in Figure 3.10.

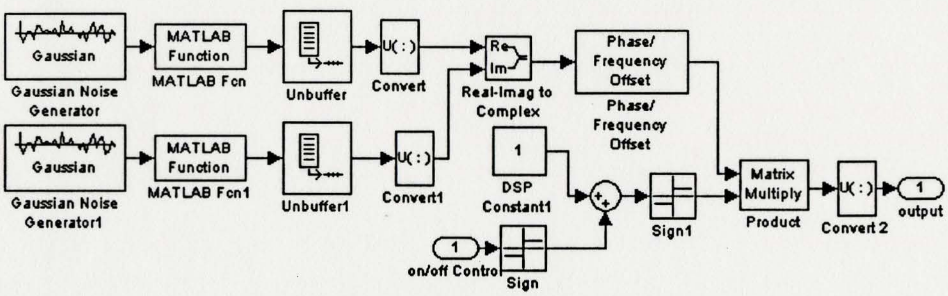

Figure 3.10: The primary user structure.

In this environment, CR users keep on monitoring and analyzing the environment spectrum usage. Once a CR has data to transmit, it has to combine its quality of service requirement with its environment learning result, and then select the spectrum holes for its transmission. The selection is based on the following points:

- The spectrum holes are currently available. This detection is based on instantaneous observations.
- Based on the spectrum holes' channel-state estimation and CR's data length to be transmitted, select the corresponding modulation method and calculate the corresponding transmit time. If the transmission rate is fixed, the transmit time is proportional to the data length.
- Based on the arrival time and service time statistics of primary users occupying those holes, estimate the non-collision probability of those holes between the CR and primary users.
- Select the holes that satisfy CR's rate requirement, with the lowest non-collision probability.

This simulation environment is generated by six primary users with different traffic patterns. We set the traffic patterns of each primary user as in Table 3.2.

Table 3.2: The parameters of legacy users.

	Inter arrival time		Service time	
	PDF	Time(ms)	PDF	Time(ms)
L1	Determinate	2.5	Determinate	1
L2	Always on	0	Always on	0
L3	Exponential	5	Exponential	2.5
L4	Exponential	2	Uniform	[0.5, 1.5]
L5	Uniform	[0.5, 5]	Uniform	[0.5, 1]
L6	Random	[1, 5]	Random	[1, 4]

In Table 3.2, PDF is the probability distribution function, T is the time range for uniform distribution or average time for Poisson process. L represents the primary user.

3.3.2 Simulation result

The CR DFS algorithm based on traffic pattern analysis improves the throughput of both CRs and primary users. Compared to the channel allocation method based on the receive signal strength only, the CR DFS algorithm reduces the collision probability and power consumption significantly. Figure 3.11 shows the power consumed by packets from CR users. With every point of CR packet length setting, the power consumption is the average value of 20 random runs with the same environment setting and random CR packet generation.

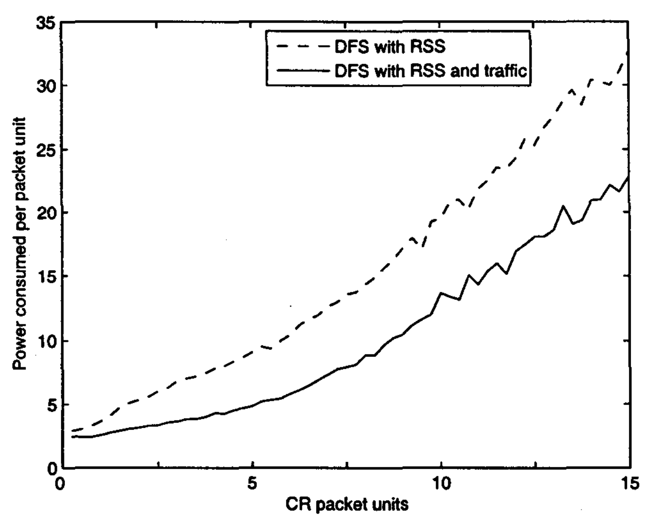

Figure 3.11: Power consumption of CR DFS with traffic analysis vs. DFS with RSS

Figure 3.12 shows the packet delay of CR users. With every point of CR packet length setting, the delay is also the average value of 20 random runs with the same environment setting and random CR packet generating. Figures 3.11 and 3.12 show that the DFS with traffic analysis performs much better than DFS with receive signal strength (RSS) detection only.

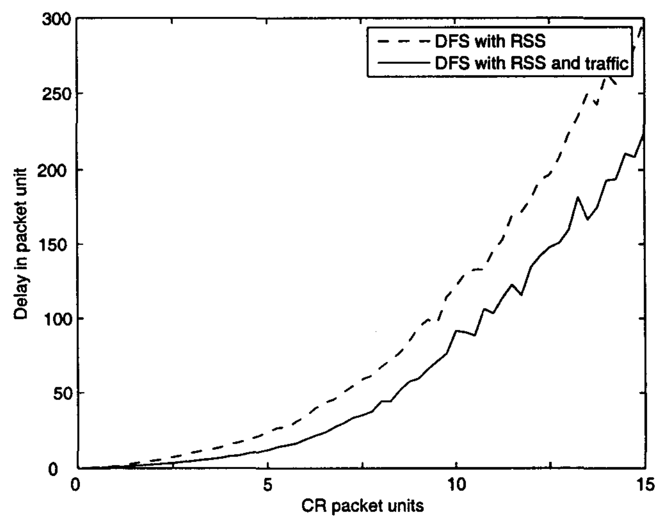

Figure 3.12: Packet delay of CR DFS with traffic analysis vs. DFS with RSS

When the packet length increases, the power consumed and the packet delay of each packet unit increase fast in a superlinear relationship with the packet length. We can see that even for a greedy CR system, its capacity is bounded by its power consumption and the quality of service which can not tolerate large delays.
Figure 3.13 shows the CR collision with primary users. With every point of CR packet length setting, the collision is also the average value of 20 random runs with the same environment setting and random CR packet generation.

Figure 3.14 shows the CR packet delay as the service-arrival ratio increases. When more data are poured into channels, the delay of CR packets increases relatively fast if using DFS without considering the traffic patterns of primary users.

Figures 3.13 shows that collisions happen more frequently as the packet length increases. When a penalty is added to a CR system from primary users according to the

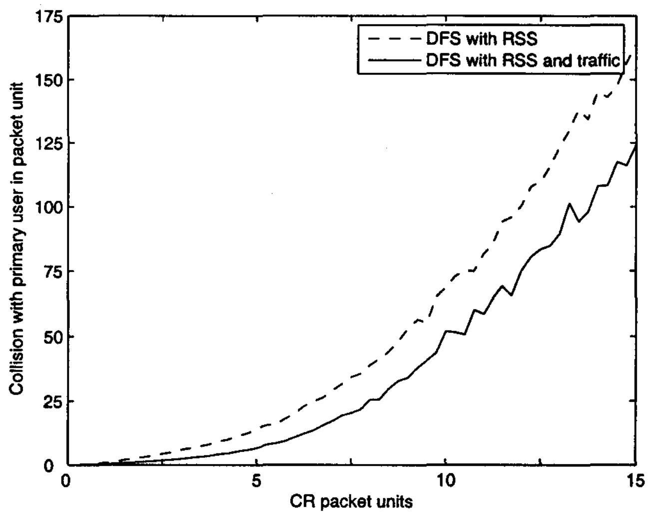

Figure 3.13: Collision of CR with DFS using traffic analysis vs. DFS using RSS

collision result, the capacity of CR system is further reduced. The power consumption and packet delay requirement from CR users plus the collision threshold required by primary users decide the CR system capacity. In (Haykin 2005), a game theoretic solution is represented for the radio resource management. It can be applied to find the optimum assignment for the collision threshold setting and the limit of a CR system in a primary user environment. This topic can be addressed as a future research topic.

Summary

In this chapter, we described a dynamic frequency selection algorithm based on traffic analysis. It is used in a CR system for its co-existing with primary users. First, traffic patterns of primary users are analyzed; then a Gaussian mixture model is introduced to represent the traffic pattern of primary users. The parameters of GMM are learned by means of the Expectation maximization algorithm. Some examples are included to illustrate the efficiency of the GMM model. Finally, the DFS algorithm using traffic analysis is applied to a CR system with a virtual wireless environment, and

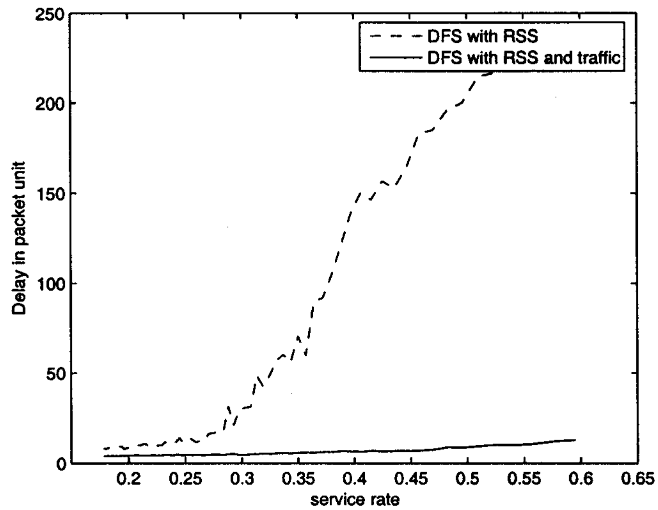

Figure 3.14: Relationship of CR Packet delay with service-arrival ratio

the simulation result shows obvious performance improvement of the CR system using our DFS algorithm.

Chapter 4

Iterative Water-Filling in the Cognitive Radio Mesh Network

Transmit power is one of the most important factors in wireless communication. It affects not only battery life, but also signal quality and interference level in a wireless system. Some examples of the importance of the transmit-power control (TPC) are:

- A near-far issue in Code Division Multiple Access(CDMA) systems.
- Satellite communication with large attenuation variance.
- Co-channel interferences in cellular systems.
- The balance of power consumption, interference, and the hop length in wireless ad hoc networks.

However, TPC itself is not a trivial problem. In a wireless mesh network, improper control of transmit power in one node of the network may have an avalanche effect in the whole network.

Unlike a wired network, transmit power in a wireless mesh network affects not only interference level, but also system delay(Kawadia and Kumar 2005). Transmit power determines both processing delays and queuing delays. The processing delay increases approximately linearly in the number of hops, which is inversely proportional to the transmit power. The queuing delay is caused by MAC contention and the interference level in the neighborhood; it increases super-linearly with the power level. The goal of TPC is to reduce end-to-end delay and increase network capacity. In low-load networks, the queuing delay is insignificant, so a high transmit power is acceptable. While in heavy traffic networks, the queuing delay is the dominant factor; it is better to select a connection mechanism that can accommodate more hops(Akyildiz, Wang, and Wang 2005).

Just like centralized control and distributed control mechanisms in previous chapters, transmit-power control can also be realized in two methods: centralized TPC and distributed TPC. In the centralized TPC, there must be a control centre, such as a base station, to control the transmit power of all subscribers in its service area. The control centre collects channel link information and sends control commands to the subscriber stations in a global optimization point of view. The centralized control mechanism is also called network-centric. The methods of centralized TPC have been discussed in many papers(Kim, Kim, Han, and Kim 2004). They require the control centre to know the radio-channel characteristics centrally. However, channel information is hard to get precisely and instantaneously; it is also difficult to fight the latency caused by transmission delays and processing delays. The exchange of channel information also causes large overhead that may not be balanced by the merit of the centralized TPC. On the other hand, in a distributed TPC mechanism, subscriber stations adjust their transmit power iteratively trying to converge to an optimal solution. It is also called user-centric TPC. Between these two extreme cases of centralized TPC and distributed TPC, another method of TPC is a hybrid version based on the joint optimization of both the network-centric and the user-centric radio resource managements. The network-centric method tries to optimize the overall performance of the network, while the user-centric method emphasizes the specific interests of individual users. This joint TPC mechanism mediates between the two extremes and manages to reach a unique Nash equilibrium by adjusting some system parameters(Feng, Mau, and Mandayam 2004). The Nash equilibrium is an optimal solution. In this way, the action selected by every user is the best response to the actions of all the other users(Haykin 2005). However, to find the optimal solution of distributed TPC is computationally intractable(Zhao 2004).

In a Wireless HUMAN mesh network, two scheduling methods are designed for the centralized control and the distributed control. For distributed schedulling, all nodes negotiate their communication parameters among their two-hop extended neighborhoods. This negotiation mechanism is the basis of distributed TPC. Our goal is to seek a good, but not necessarily optimal, distributed TPC solution so that in an interference environment, rate requirements of all links in the CR mesh network are satisfied using the OFDMA physical layer protocol.

In an OFDMA system, each symbol contains multiple users. The system performance is heavily dependent on the mismatch conditions such as frequency offsets(Moose 1994). In an OFDMA system, users must be aligned in both the time-domain and frequency-domain to keep orthogonality, which is an inherent characteristic of OFDMA. However, the frequency offset is hard to be eliminated and can be introduced by many sources, such as oscillator inaccuracy, frequency jitter or Doppler shift. In an infrastructure network, the method of synchronization among different users in uplink is discussed in(van de Beek, Borjesson, Boucheret, Landstrom, Arenas, Ostberg, Wahlqvist, and Wilson 1999). All users adjust their local clocks and frequencies according to the base station. However, in an ad-hoc network, the network is decentralized, so lack of orthogonality between sub-carriers in a multi-user OFDMA system becomes a serious issue. Although with a long enough cyclic prefix, inter-symbol interference can be overcome, inter-channel interference can not be counteracted easily. Even using an ideal brick-wall filter, the connections in an OFDMA system still compete with each other to achieve their individual capacities.

4.1 Iterative Water-Filling Algorithm

In his PhD thesis(Yu 2002), Yu introduced an iterative water-filling (IWF) algorithm to solve crosstalks that impact the performance of digital subscriber line systems. In a digital-subscriber-line system, different users transmit on the same frequency band and the bandwidth is fixed. The inter-user interference is caused by near-end crosstalk or far-end crosstalk. In a cognitive radio mesh network, interferences come from inter-channel interference (ICI) and co-channel interference. In this thesis, we use the IWF algorithm for distributed TPC in a CR mesh network with OFDMA physical layer. Our goal is to find a power vector such that channels are used as less as possible with desired data rates and power constraints. Compared to (Wong, Cheng, Letaief, and Murch 1999), the computational complexity of IWF algorithm is much lower.

4.1.1 Rate constraints

Different users require different transmission rates. A transmission rate is closely related to signal-to-interference-noise ratio (SINR) requirement. Radio resource management in a CR mesh network is a combined data rate and power-control problem. Rate requirement $r_{i,min}$ should satisfy $r_{i,min} \leq f(\gamma_i)$, where f denotes a function and γ_i is the SINR of the receiver i(Zhao 2004).

$$\gamma_i(\mathbf{P}) = \frac{g_{ii}p_i}{\sum\limits_{j=1;j\neq i}^{Q} g_{ij}p_j + n_i} \tag{4.1}$$

where g_{ii} is the path loss from transmitter i to receiver i. g_{ij} is interference factor from transmitter j to receiver i, n_i is background noise of receiver i, and p_i is the transmit power of transmitter i. The maximum transmit power vector is $\mathbf{S} = (S_1, S_2, \cdots, S_Q)$, where S_i is the maximum transmit power of transmitter i.

The goal of TPC is to minimize the power $\mathbf{P}$ and the number of subchannels Q subject to

$r_i(\mathbf{P}) \geq r_{i,min}$

According to the Shannon channel capacity theorem for a band-limited channel, the relationship between the data rate r and the SINR γ is defined by

$$r = c' \log(1 + \frac{\gamma}{\Gamma}) \tag{4.2}$$

where Γ is an SNR gap that relates to the bit error rate requirement(Haykin 2005). Suppose that we have 2 transmitters and 2 receivers and the channels are additive white Gaussian interference channels; then the receive signals can be calculated as:

$$\begin{aligned} \mathbf{y}_1 &= \mathbf{A}_{11}\mathbf{x}_1 + \mathbf{A}_{12}\mathbf{x}_2 + \mathbf{n}_1 \\ \mathbf{y}_2 &= \mathbf{A}_{22}\mathbf{x}_2 + \mathbf{A}_{21}\mathbf{x}_1 + \mathbf{n}_2 \end{aligned} \tag{4.3}$$

where $\mathbf{A}_{11}$ and $\mathbf{A}_{22}$ denote channel attenuations caused by the distance of transmitter and receiver pairs. $\mathbf{A}_{12}$ and $\mathbf{A}_{21}$ are attenuated inter-channel interference factor caused by the distance and parameter mismatch. We suppose that each sub-channel follows flat fading, but in the whole band the channel is a select-fading channel; then the TPC problem can be formulated as

$$\min \mathbf{S}, \mathbf{Q} \tag{4.4}$$

subject to

$$\begin{bmatrix} P_1^{(R)}(f) \\ P_2^{(R)}(f) \end{bmatrix} = \begin{bmatrix} g_{11}(f) & g_{12}(f) \\ g_{21}(f) & g_{22}(f) \end{bmatrix} \begin{bmatrix} P_1^{(T)}(f) \\ P_2^{(T)}(f) \end{bmatrix} + \begin{bmatrix} N_1(f) \\ N_2(f) \end{bmatrix} \tag{4.5}$$

with

$$\begin{aligned} g_{11} &= \frac{\beta}{d_{11}^n} \\ g_{12} &= A_1 \frac{\beta}{d_{12}^n} \\ g_{21} &= A_2 \frac{\beta}{d_{21}^n} \\ g_{22} &= \frac{\beta}{d_{22}^n} \end{aligned} \tag{4.6}$$

where A_1 is the interference factor of the first transmitter to the second receiver, while A_2 is the interference factor of the second transmitter to the first receiver. Solving Eqs. 4.4 through 4.6 yields the following formulas:

$$\gamma_1 = \frac{g_{11}P_1^T}{g_{12}P_2^T + N_1} \quad \gamma_2 = \frac{g_{22}P_2^T}{g_{21}P_1^T + N_2} \tag{4.7}$$

where γ_i is SINR.

$$r_j = c\log(1 + \frac{\gamma_j}{\Gamma}) \tag{4.8}$$

and this rate should satisfy the constraint

$$r_j \geq r_{j,min} \tag{4.9}$$

4.1.2 Iterative water-filling algorithm

The transmit power can be adjusted iteratively to achieve the multiple-access rate requirement of each link. In (Yu 2002), if the solution condition is satisfied, the iterative water-filling algorithm is able to converge to a limit point from any initial assignment of transmit power P_i. The limit point maximizes the sum capacity of a Gaussian vector multiple access channel. The iterative water filling algorithm converges fast. The converge speed is related to the number of users and the number of channels occupied by each user. The main objective of TPC in a CR mesh network is to characterize the pure-strategy Nash equilibria in an interference channel game. At the Nash equilibrium, the strategy of each user is an optimal response to the strategies of other players.

The IWF TPC algorithm includes two-loops of water-filling steps:

- Fixing $P_{-i}(f)$, the optimal $P_i(f)$ must be the solution to the following optimization problem:

$$\begin{gathered}\min f_{band}, p_i(f) \\ s.t. \\ \int_{f_{band}} \log_2\left(1+\frac{g_{ii}p_i(f)}{n_i(f)+\sum\limits_{j,j\neq i}\alpha_{ji}(f)g_{ji}p_j(f)}\right)df \geq r_{i,min} \\ i=0,1,\cdots,K\end{gathered} \tag{4.10}$$

  with $p_i(f)$ is the power allocated to the user i. $p_{-i}(f)$ is the power allocated to other users except user i. g is the channel attenuation, and α is the interference factor. r_{min} is the minimum rate requirement. K is the number of users. At the start of iteration, the transmit powers of all users are set to zero.

- Inner loop (Water-filling). Starting with the first user, the users perform the water-filling process, subject to their own power constraint. They will try to employ as small a number of channels as possible to satisfy their data-rate requirement. In addition to background noise, the water-filling computation accounts for interference produced by the other users.

- Outer loop (Power adjustment). After the inner iteration is completed, the powers allocated to the users are adjusted: the power is reduced for those users with higher actual data-transmission rate than their target rate, and increased for those users with inverse scenario, subject to their power constrain.

- Confirmation step. The transmission data rates of all users are checked after the power adjustment. If the target rates of all users are satisfied, the computation is terminated. Otherwise, the algorithm goes back to the inner loop, and the computation is repeated.

4.1.3 An example of iterative water-filling

Here is an example of TPC with three users. We use Yu's IWF algorithm. Suppose we have 9 channels available, and the pair 1(transmitter 1 to receiver 1) can use channel index [1,3,7], while pair 2(transmitter 2 to receiver 2) can use channel index [2,5,6], and pair 3(transmitter 3 to receiver 3) can use channel index [4,8,9]. An example of the path loss matrix G may look like

$$\begin{bmatrix} 0.3229 & 0.0032 & 0 & 0.0018 & 0.0012 & 0.0015 & 0 & 0.0029 & 0.0008 \\ 0.0020 & 0.8450 & 0.0010 & 0.0014 & 0 & 0 & 0.0013 & 0.0021 & 0.0005 \\ 0 & 0.0029 & 0.3372 & 0.0018 & 0.0007 & 0.0014 & 0 & 0.0020 & 0.0019 \\ 0.0028 & 0.0006 & 0.0023 & 0.6678 & 0.0002 & 0.0034 & 0.0016 & 0 & 0 \\ 0.0011 & 0 & 0.0025 & 0.0016 & 0.8329 & 0 & 0.0025 & 0.0036 & 0.0009 \\ 0.0016 & 0 & 0.0019 & 0.0007 & 0 & 0.8393 & 0.0002 & 0.0039 & 0.0025 \\ 0 & 0.0008 & 0 & 0.0035 & 0.0039 & 0.0016 & 0.3237 & 0.0005 & 0.0030 \\ 0.0022 & 0.0006 & 0.0014 & 0 & 0.0017 & 0.0002 & 0.0031 & 0.6753 & 0 \\ 0.0000 & 0.0036 & 0.0023 & 0 & 0.0038 & 0.0008 & 0.0003 & 0 & 0.6863 \end{bmatrix} \quad (4.11)$$

The rate constrain is $[9, 9, 6] bits/symbol$. Power constraint is $0dB$. The iterative water-filling result, obtained in ***5*** iteration, is shown in Fig.4.1.

4.2 Inter-Channel Interference of OFDMA Mode

An OFDM method is robust with frequency-selective fading and it is highly spectrally efficient. Because of this attribute, OFDM has been widely proposed for both broadcast systems, like digital audio broadcast and digital video broadcast, and multiple-access wireless systems, like IEEE 802.11a and IEEE 802.16a. OFDM is an efficient way of modulation. However, even for the single-user or broadcast scenarios, it is well known that OFDM is very sensitive to frequency/time offsets, which destroy orthogonality among sub-carriers and thereby cause inter-channel interference. It is

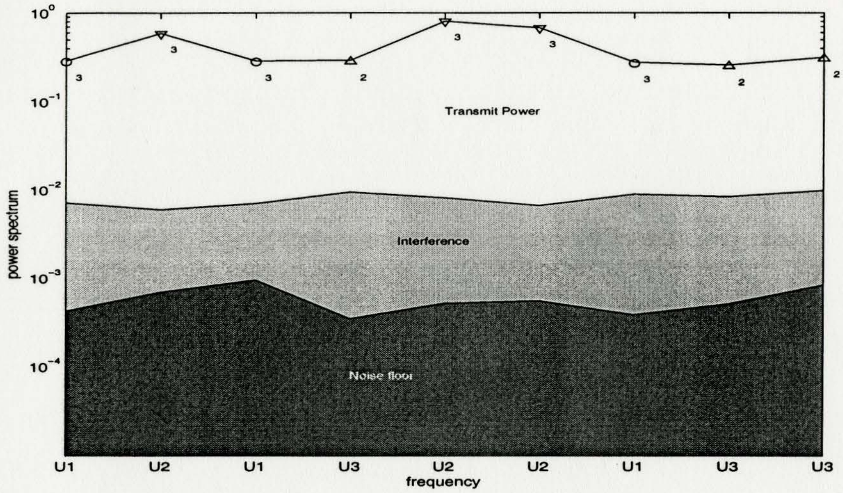

Figure 4.1: Iterative water filling

even more challenging for OFDMA techniques, since multiple users share one OFDM symbol simultaneously. Figure 4.2 shows an OFDMA snapshot in a three-user case. The solid curve shows no frequency offset, while the dotted curve and the dashed curve show 3% frequency offset relative to the carrier space. From this figure, we see that the amplitude is reduced because of the frequency offset, and orthogonality among sub-carriers is destroyed.

In (Moose 1994), Moose demonstrated that to maintain a signal-to-interference ratio of 20dB, the frequency offset should be limited to 4% or less of the inter-carrier space. The frequency offset in OFDM systems causes the amplitude reduction and inter-channel interference. As mentioned previously, frequency offset is caused by oscillator tuning mismatch, frequency jitter, mobile Doppler shift or combination thereof. To counteract the impact of frequency offset, some techniques such as interleaving, coded-OFDM and multi-tapper frequency domain equalizer have to be

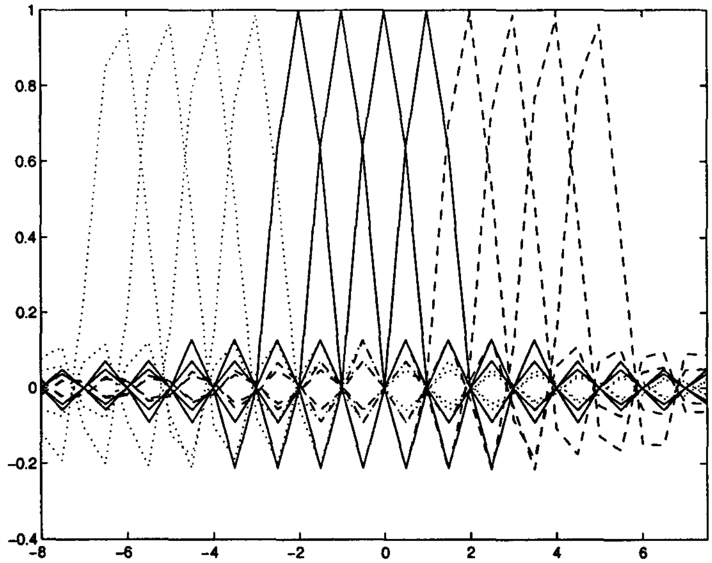

Figure 4.2: The impact of the frequency offset in OFDM

adopted and incorporated in an automatic frequency controller in receiver.

An OFDM symbol is generated by the inverse discrete Fourier transform,

$$x_n = \frac{1}{N} \sum_{k=-K}^{K} X_k e^{2\pi jnk/N} \tag{4.12}$$

with $n = 0, 1, 2, \cdots, N-1$, and $N \geq 2K+1$

The individual sinusoids are orthogonal in one symbol interval; that is

$$\sum_{n=0}^{N-1} x_{nk} x_{nl}^* = (1/N)|X_k|^2 \delta_{kl} \tag{4.13}$$

where $x_{nk} = (1/N)X_k e^{2\pi jnk/N}$ and '*' denotes the complex conjugation. δ_{kl} is the Kronecker delta function.

The actual transmit signal is an N-point OFDM symbol with a cyclic prefix of length N_g samples, which is also called guard interval, as shown in the sequence

$$\{x_{N-N_g}, \cdots, X_{N-2}, x_{N-1}, x_0, x_1, \cdots, x_{N-1}\} \tag{4.14}$$

The length of the guard interval should be greater than or equal to the time spread of the channel. If this condition is satisfied, the symbol is extended periodically through the cyclic prefix, and the orthogonality of the carrier is maintained over one symbol period; the inter-channel interference is thereby eliminated. At the same time, with this guard interval, the inter-symbol interference can also be eliminated. Since the insertion of a guard interval reduces the channel throughput, it cannot be set too long. If the guard interval is shorter than the time spread of the channel, some techniques such as time-domain equalizer would have to be used to shorten the channel impulse response before the DFT demodulation procedure.

When the OFDM symbol passes through a channel with proper synchronization, the received signal is defined by

$$y_n = \frac{1}{N} \sum_{k=-K}^{K} X_k H_k e^{2\pi jn(k+\epsilon)/N} + w_n \tag{4.15}$$

Here H_k is the channel response at the k^{th} frequency bin, and ϵ is the relative frequency offset, the frequency offset over the carrier space. w_n is the complex envelop of the additive white Gaussian noise(AWGN).

Without including a compensator for the frequency offset, after removing the guard samples, demodulation is realized by the discrete Fourier transform

$$Y_k = \sum_{n=0}^{N-1} y_n e^{-2\pi jkn/N} \tag{4.16}$$

In addition to the signal in that band and the AWGN, the frequency offset between the transmitter and receiver also causes the inter-channel interference. Y_k can be represented as the sum of three components(van de Beek, Borjesson, Boucheret, Landstrom, Arenas, Ostberg, Wahlqvist, and Wilson 1999).

$$Y_k = (X_k H_k)\{(\sin(\pi\epsilon)/[N\sin(\pi\epsilon/N)]\}e^{j\pi\epsilon(N-1)/N} + I_k + W_k \tag{4.17}$$

The first component is the reduced amplitude caused by the frequency offset. The second component, I_k, is the inter-channel interference, which is defined by(van de Beek, Borjesson, Boucheret, Landstrom, Arenas, Ostberg, Wahlqvist, and Wilson 1999)

$$I_k = \sum_{l=-K, l \neq k}^{K} (X_l H_l)\{(\sin(\pi\epsilon)/[N\sin(\pi(l-k+\epsilon)/N)]\} e^{j\pi\epsilon(N-1)/N} e^{-j\pi(l-k)/N} \quad (4.18)$$

The third component, W_k, is the AWGN.

Under the assumption of zero mean and no correlation in the X_k signal, the statistics of interference in channel k polluted by channel l can be represented as

$$\mathrm{E}[I_k] = 0 \quad (4.19)$$

with E denotes the expectation operator. and

$$\mathrm{E}[I_{lk}^2] = |X_l|^2 |H_{lk}|^2 \frac{[\sin(\pi\epsilon)]^2}{[N\sin(\pi(l-k+\epsilon)/N)]^2} \quad (4.20)$$

In a single link, the ICI can be compensated for by a frequency controller. When using OFDMA techniques, the inter-channel interference phenomenon becomes severe since the automatic-frequency-control mechanism cannot compensate for other links. If the maximum frequency offset allowed in a system is ϵ_{max}, then the relative frequency offsets of a receiver to a transmitter follows a random distribution in a range of $[-2\epsilon_{max}, 2\epsilon_{max}]$.

In our experiment, we assume that all the transceiver pairs are well synchronized in the time domain, so that the guard interval could eliminate the inter-symbol interference. If the frequency offset is zero, then the inter-channel interference does not exist. In each frequency bin, the channel is approximated as a flat-fading channel with a scalar gain only. The received SINR on sub-carrier i is defined by

$$\gamma_i(S) = \frac{g_{ii} p_i}{\sum_{j=1; j \neq i}^{Q} g_{ji} p_j + n_i} \quad (4.21)$$

Here the gain includes the channel gain H and the frequency offset effects; n_i is the complex AWGN. g_{ii} is a path loss of the same frequency bin and it is defined by

$$g_{ii} = |H_{ii}|^2 \left| \frac{\sin(\pi\epsilon_{ii})}{N\sin(\pi\epsilon_{ii}/N)} \right|^2 \tag{4.22}$$

g_{ji} is the inter-channel interference from frequency bin j to bin i and it is defined by

$$g_{ji} = |H_{ji}|^2 \left| \frac{\sin(\pi\epsilon_{ji})}{N\sin(\pi(j-i+\epsilon_{ji})/N)} \right|^2 \tag{4.23}$$

Here ϵ_{ji} denotes the normalized frequency offset between the transmitter on channel j and the receiver on channel i.

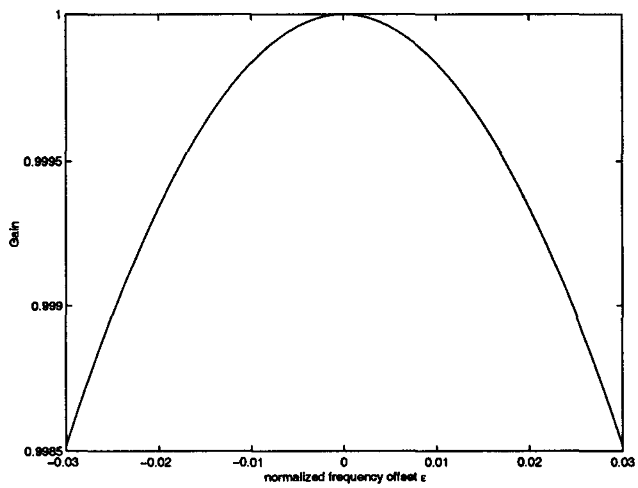

Figure 4.3: The impact of the frequency offset of the same bin in OFDMA

Figure 4.3 shows the signal attenuation caused by the frequency offset, and Figure 4.4 shows the inter-channel interference caused by the frequency offset.

In a CR mesh network, the interference caused by the frequency offset from neighbors on adjacent channels can be very severe. If the received signal is very weak (i.e. the desired transmitter is far away), and the strong interfering transmitter is just nearby,

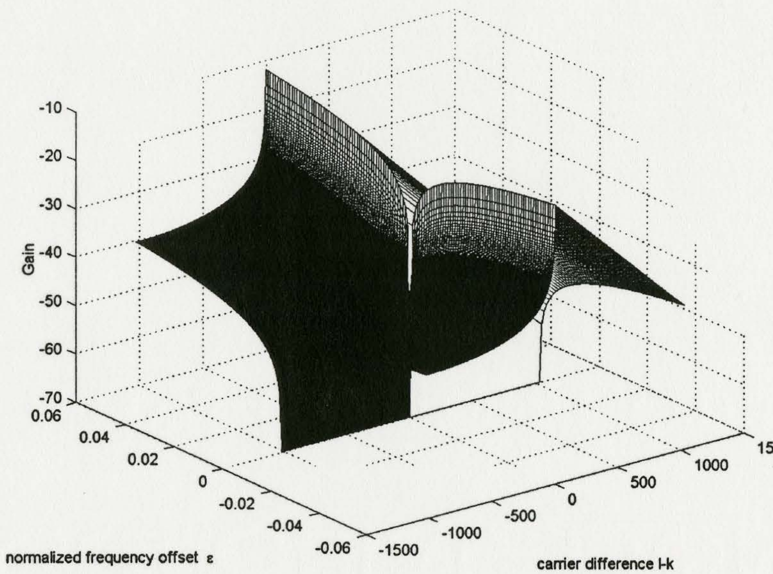

Figure 4.4: The impact of the frequency offset of the different Bin in OFDM

the SINR in this case can be very low. So we have to figure out possible solutions for this issue.

For the mesh network of OFDMA method in 802.16a, the frequency offset is required to be within ±3% of the carrier space. This causes the maximum frequency difference to be ±6% of the carrier space between transmitter and receiver pairs. Although transmit-receiver pair could adjust the carrier offset between them to compensate the power attenuation caused by the carrier offset, the transmission from other pairs still cause the interchannel interference to the pair interested. One solution is to use transmit-power control.

4.3 Transmit-Power Control in OFDMA Mode

With embedded intelligence, a CR can "listen" to huge swaths of the spectrum and determine which chunks of the spectrum are available. Our experiment is based on the broadband wireless metropolitan area network environment. There are a large

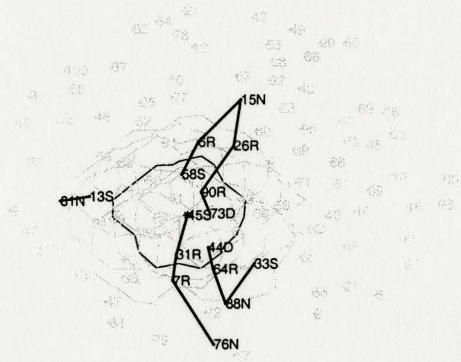

Figure 4.5: Iterative water filling configuration around node 45

number of frequency bands which are divided into 2048 frequency bins called subcarriers. CRs in this network could share the spectrum if the primary licensees in that spectrum, such as radar and TV transmitters, are not using it at that time or in that place.

The CRs are self-organized in a mesh network. In a CR mesh network, mesh BS nodes connect to the internet or other network backhaul. BSs can work as a data source, sink, or both. Other nodes are SS nodes which can work as a data source, a data sink, or a relay point. Figure 4.5 shows an instantaneous link status in the mesh network around node 45.

The nodes inside the black contour are the neighbors of node 45, and the nodes covered by the gray contours belong to the extended neighborhood of node 45. Nodes 15, 81, 88, and 76 are mesh BSs, denoted with N; nodes 44 and 73 are the link sinks, denoted by D; and nodes 45, 33, 13, and 58 are the link sources, denoted by S. The other nodes with notation R are the relay nodes.

Suppose that the other links are already established and are working properly; we use the link from 45 to 76 by way of nodes 31 and 7 to illustrate the IWF procedures in the mesh network.

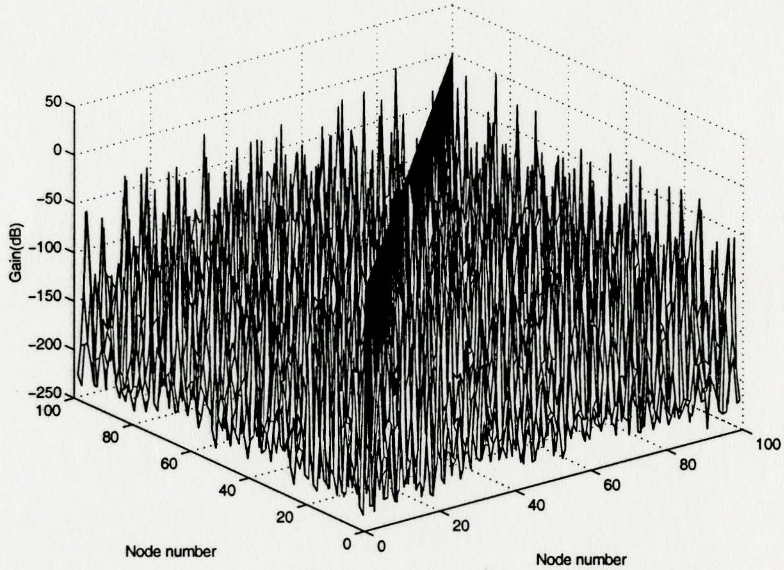

Figure 4.6: The path gain of the mesh network

Before the link 45-31-7-76 is established, the transmit power and rate of the other links are assumed to be stable. We use the global information to find the stable operating point.

Channels are modeled as exponential path loss and log-normal shadow fading channels(Goldsmith 2005), with the path loss being

$$PL(d)[dB] = PL(d0) + 10nlog(d/d0) + X_c \tag{4.24}$$

The environment path loss exponent $n = 4$ and $X_c \propto N(0, \sigma_p)$ with $\sigma_p = 3.5$(Blogh, Cherriman, and Hanzo 2001b)(Blogh, Cherriman, and Hanzo 2001a). The path gain between different nodes is shown in Figure 4.6

Because of the frequency-offset between different transmitter nodes and receiver nodes, orthogonality of the subcarriers is not maintained and inter-channel interference is therefore introduced. For the transmitter and receiver pair T_i and R_i, we may show that the channel gain of each frequency bin is

$$P_r(c_{i,k}) = P_t(c_{i,k})G_{i,i}\left|\frac{\sin(\pi * \epsilon_i)/N}{\sin(\pi * \epsilon_i/N)}\right|^2 \tag{4.25}$$

Here $P_r(c_{i,k})$ is receive signal power of node R_i on channel $c_{i,k}$, which belongs to the link pair i and it is the k^{th} allocated sub-carrier. $P_t(c_{i,k})$ is the transmit-power of node T_i on channel $c_{i,k}$. $G_{i,i}$ represents the path loss and shadow fading from T_i to R_i. ϵ_i is the frequency difference between transmitter T_i and receiver R_i. N is the FFT size.

The other transmitters are the interference sources to receiver R_i. We may show that the interference level of the channel $c_{i,k}$ is

$$P_{rI}(c_{i,k}) = \sum_{j,j \neq i or l \neq k} G_{i,j} \sum_{c_{j,l} \in T_j} P_t(c_{j,l})\left|\frac{\sin(\pi * \epsilon_{ij})/N}{\sin(\pi * (c_{i,k} - c_{j,l} + \epsilon_{ij})/N)}\right|^2 \tag{4.26}$$

Here $P_{rI}(c_{i,k})$ is the received interference of node R_i on channel $c_{i,k}$. T_j denotes the other transmitters except the transmitter T_i or the transmitter T_i on the channels other than $c_{i,k}$. $G_{i,j}$ represents the path loss and shadow fading from transmitter T_j to receiver R_i, ϵ_{ij} is the frequency difference between transmitter T_j and receiver R_i. $c_{j,l}$ belongs to the link pair j and it is the l^{th} allocated sub-carrier.

The maximum transmit-power mask is regulated so that the out-of-band interference may not exceed the interference mask. Also each link has its minimum rate requirement. The goal of the IWF is to allocate each link with minimum bandwidth, minimize its transmit power, and satisfy its rate constraint.

The FFT size is 2048, representing 2048 subcarriers to be shared by the mesh network. For compatibility with other wireless systems, the guard bands are required on both sides of this bandwidth. As in 802.16a, we adopt 176 subcarriers on the low-frequency side of the band as the guard band, and 175 on the high-frequency side. The carriers are allocated as in Table 4.1.

Parameter	Value
Number of DC carriers	1
Number of guard carriers(low)	176
Number of guard carriers(high)	175
Used number of carriers	1696
Total number of carriers	2048
Number of subchannels	32
Number of used carriers	53
Number of data carriers in subchannel	48
Number of pilot carriers in subchannel	5

Table 4.1: Carrier allocation in the mesh network

In Figure 4.5, before node 45 initiates data transfer, there are 9 links existing in the extended neighborhood of node 45 as shown in Table 4.2.

Link	transmitter-receiver
1	58,6
2	6,15
3	15,26
4	26,90
5	90,73
6	64,44
7	88,64
8	33,88
9	13,81

Table 4.2: Links in the neighborhood of node 45

Before a new link is established, the current system with 9 links works in a stable state as shown in Table 4.3. The power resolution is 2dB.

The new link establishment procedure uses the IWF algorithm to find a stable power assignment. This method follows Yu's IWF algorithm, and goes through the following phases:

Link	Name	Subchannels	Rate	Max TxPower(dB)
1	58S-6R	21	131	-28
2	6R-15N	23	141	-8
3	15N-26R	10	135	-20
4	26R-90R	3	136	-12
5	90R-73D	15	132	-42
6	64R-44D	25	143	-46
7	88-64R	16	129	-24
8	33S-88	30	132	-14
9	13S-81N	20	141	-44

Table 4.3: Stable status before the new link is established

1. The new link uses average SNR in subchannels to find which subchannel the link can use. Then the link uses the water-filling algorithm to find the number of subchannels that fit the rate requirement and get the maximum possible rate within the power restrictions. The results of this step are shown in Table 4.4. In this step, the algorithm that introduces a new link assigns its power in a greedy way.

Link	Name	Subchannels	Rate
10	45S-31R	7	228

Table 4.4: Iterative water-filling step1 in the mesh network

2. The newly active link disturbs the current stable link setup. Pre-existing links have to check their rate status. With a $6dB$ margin, the rates of previous links drop significantly as is shown in Table 4.5. Those links that could not satisfy their rate requirement have to adjust their power in a greedy method. Bit allocations of links are also changed based on the new interference noise situation. This causes a big power assignment change in the current system. The results obtained are shown in Table 4.5.

Link	Name	Subchannels	DropedRate	NewRate	Max NewPower (dB)
1	58S-6R	21	87	240	0
2	6R-15N	23	108	159	0
3	15N-26R	10	90	238	0
4	26R-90R	3	81	188	0
5	90R-73D	15	9	288	0
6	64R-44D	25	110	210	0
7	88-64R	16	91	204	0
8	33S-88	30	93	185	0
9	13S-81N	20	91	252	0
10	45S-31R	7	228	228	0

Table 4.5: Iterative water-filling step2 in the mesh network

3. After the rates of all links are satisfied, the links reduce their power in 2dB steps to reduce power consumption and reduce interference. The results obtained are shown in Table 4.6.

Link	Name	Subchannels	Rate	Max NewPower (dB)
1	58S-6R	21	131	-28
2	6R-15N	23	141	-8
3	15N-26R	10	135	-20
4	26R-90R	3	134	-12
5	90R-73D	15	139	-40
6	64R-44D	25	143	-46
7	88-64R	16	129	-24
8	33S-88	30	132	-14
9	13S-81N	20	141	-44
10	45S-31R	7	136	-26

Table 4.6: Iterative water-filling step3 in the mesh network

Just like the establishment of hop 45-31, the other two hops are established. When the entire link 45-31-7-76 is established, all links of the system will settle according to Table 4.7.

Link	Name	Subchannels	Rate	Power
1	58S-6R	21	144	-26
2	6R-15N	23	141	-8
3	15N-26R	10	135	-18
4	26R-90R	3	131	-12
5	90R-73D	15	135	-40
6	64R-44D	25	144	-46
7	88-64R	16	129	-24
8	33S-88	30	132	-14
9	13S-81N	20	141	-44
10	45S-31R	7	138	-26
11	31R-7R	10	131	-36
12	7R-76D	21,2,18	138	-6

Table 4.7: Iterative water-filling with a new links in the mesh network

The stable status of the link setting is in its Nash equilibrium based on its IWA strategy. No link can get better performance if other links keep their channel occupation and power assignments unchanged. The introduction of a new link greatly disturbs its neighbors, and the degraded SNR may cause links to drop. To compensate for this problem, we modified the greedy part of the IWA to make the link status change slightly.

Our new IWA method slightly modifies Yu's IWF algorithm. Our modified IWF algorithm controls the SNR drop within a 2dB range so that the margin can be better than 4dB. The new link will use a minimum number of channels and minimum power to satisfy its rate requirement. If a new link establishment will cause a drop in a current links' SNR margin to be less than 2dB, it will be permitted by its neighbors, and the link will be established. Otherwise, the new link will try other sub-channels for its establishment. After the new link is established, all links will adjust their power in a step-by-step manner to compensate for the SNR margin gap. When the new link establishment uses the modified iterative water-filling algorithm to find a stable power assignment, it goes through the following phases:

1. First, the introduction of a new link assigns its power in a 'just satisfied' way shown in Table 4.8.

Link	Name	Subchannels	Rate	Power
10	45S-31R	7	136	-28

Table 4.8: Modified IWF step1 in the mesh network

2. The active new link also causes disturbance of the current stable link setup. Previous links have to check their rate status, given a $4dB$ margin. If the rate is not satisfied, the new link has to move to other subchannels or use more channels with lower transmit power. The results obtained are shown in Table 4.9.

Link	Name	Subchannels	Rate check(4dB margin)
1	58S-6R	21	pass
2	6R-15N	23	pass
3	15N-26R	10	pass
4	26R-90R	3	pass
5	90R-73D	15	pass
6	64R-44D	25	pass
7	88-64R	16	pass
8	33S-88	30	pass
9	13S-81N	20	pass
10	45S-31R	7	pass

Table 4.9: Modified IWF with 4dB margin rate check

3. After the rates of all links are satisfied, the new link is granted and all links have to adjust gradually for SNR margin compensation as shown in Table 4.10.

Just like the establishment of hop 45-31, the other two hops are established. When the entire link 45-31-7-76 is established, all links of the system settle into the status shown in Table 4.11.

Link	Name	Subchannels	Rate(6dB)	NewRate	Max NewPower (dB)
1	58S-6R	21	131	131	-28
2	6R-15N	23	141	141	-8
3	15N-26R	10	126	135	-18
4	26R-90R	3	134	134	-12
5	90R-73D	15	132	132	-42
6	64R-44D	25	143	143	-46
7	88-64R	16	128	128	-24
8	33S-88	30	132	132	-14
9	13S-81N	20	141	141	-44
10	45S-31R	7	136	136	-28

Table 4.10: Modified IWF step3 in the mesh network

Link	Name	Subchannels	NewRate	Max NewPower (dB)
1	58S-6R	21	131	-28
2	6R-15N	23	141	-8
3	15N-26R	10	134	-18
4	26R-90R	3	133	-12
5	90R-73D	15	132	-42
6	64R-44D	25	143	-46
7	88-64R	16	132	-22
8	33S-88	30	132	-14
9	13S-81N	20	141	-44
10	45S-31R	7	136	-28
11	31R-7R	20	147	-36
12	7R-76D	10,21,2	134	-6

Table 4.11: Modified IWF with a new links in the mesh network

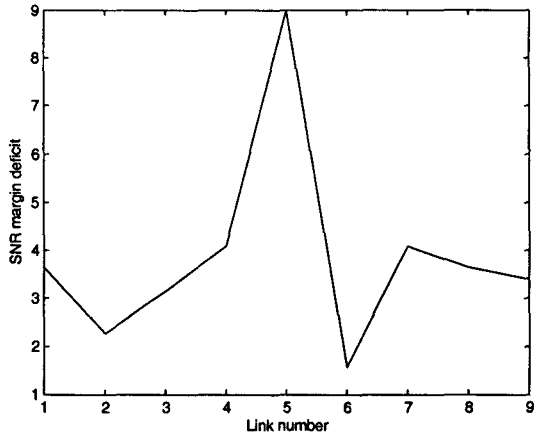

Figure 4.7: SNR deterioration using original IWF algorithm

An experiment is used to compare Yu's original IWF algorithm with the modified IWF algorithm. In the experiment, links in the wireless mesh network are established randomly. The original IWF algorithm and the modified IWF algorithm are applied in the experiment to find how many iterations are required for a new link to be established. The experiment result is shown in figure 4.9, 4.10, and 4.11. The result shows that the modified IWF algorithm could spend more iterations for the system to reach its Nash equilibrium. However the SNRs of existing links never drop more than 2dB.

As Yu illustrated in (Yu 2002), the original IWF algorithm is a good and fast distributed TPC solution. However as a new link added, the current links are changed dramatically. Although the links settled down fast, the deterioration of SNR in a short period may cause links to drop. In the previous experiment, when the new link 45-31 is added to the system, the worst temporary SNR drops 9dB as shown in Figure 4.7.

The modified IWF algorithm is based on the original IWF algorithm, but is adjusted to prevent the large SNR change. It protects the current links' signal quality.

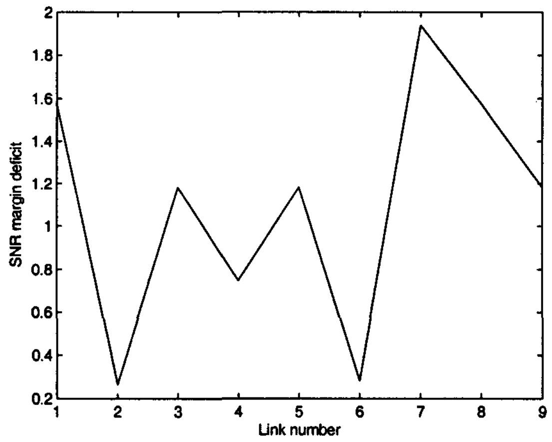

Figure 4.8: SNR deterioration using modified IWF algorithm

The SNR margin is always above 4dB as shown in Figure 4.8. However, the modified IWF prolongs the system settle down time. It also settles in a Nash equilibrium. Figure 4.9 shows the average settle down time for the original IWF algorithm. It shows that the iteration time to add a new link does not change with the number of links.

Figure 4.10 shows the average number of iterations to add a new link using the modified IWF algorithm. It shows that the iteration time to add a new link does not change with the number of links.

However, Figure 4.11 shows the average number of iterations needed for the system to settle down after adding a new link using the modified IWF algorithm. It shows that the iteration time does increase with the number of links.

In (Haykin 2005), Haykin discussed the TPC algorithm in a CR system based on game theory. The IWF algorithm is based on cooperation among CR users. It is fast

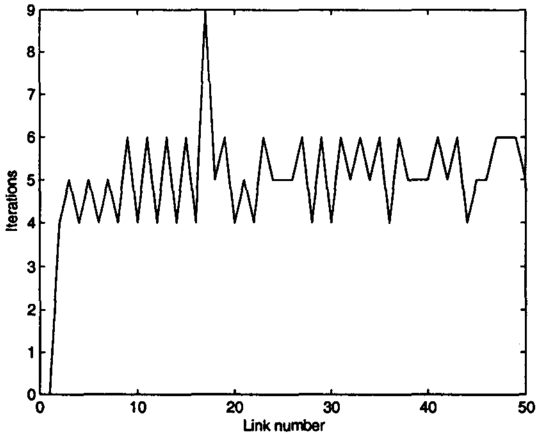

Figure 4.9: Iteration number for adding a new link using original IWF algorithm

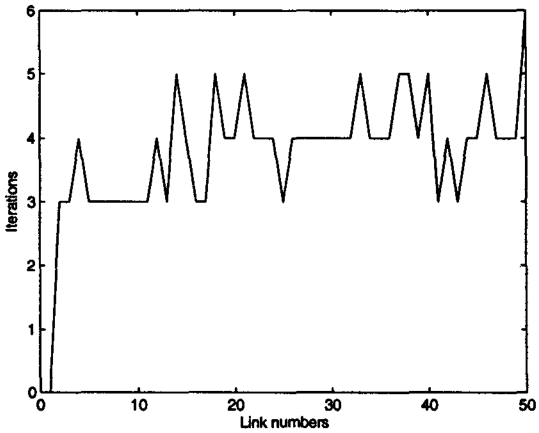

Figure 4.10: Iteration number for adding a new link using modified IWF algorithm

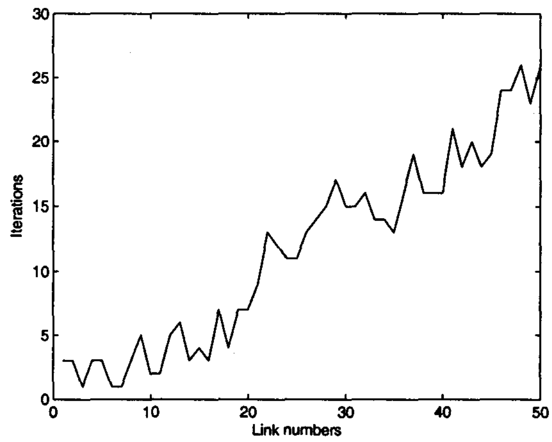

Figure 4.11: Iteration number for adjusting power using modified IWF algorithm

but can not solve the exploitation posed by greedy users. The TPC algorithm based on game theory is slow but it is able to solve the exploitation problem. The combination of these two algorithms is a future direction of TPC in a CR mesh network.

Summary

In this chapter, we discussed the importance of transmit-power control in a CR mesh network. Then we introduced the existence of interference in a CR mesh network with OFDMA physical layer. The iterative water-filling is selected to solve the distributed transmit-power control issue in the CR mesh network. When a new link is added, to avoid the SNR deterioration of current links, the iterative water-filling algorithm is modified to suit the CR mesh network. Finally, a comparison of the original iterative water-filling algorithm and the modified iterative water-filling algorithm is presented in this thesis.

Chapter 5

Conclusions

In this thesis, we have addressed three major issues pertaining to the study of cognitive radio: mesh networks, dynamic frequency-selection, and transmit-power control. In each of these areas, through sensible experiments, we have come up with some important conclusions that are summarized as follows:

1. Wireless mesh networks.

The physical layer realization of our CR mesh network is based on the OFDMA mechanism in IEEE802.16a standard. This is well-suited for the application of CR since CR is introduced to co-exist with primary users and operate on spectrum holes. The IEEE standard and the use of Simulink models provide the tools needed to simulate the CR physical layer for real-life applications. The use of mesh signalling provides a path for cooperation among CR users. Specifically, given a number of CR users, we demonstrated the use of mesh signalling to exchange user configurations, granting new nodes, and informing the users' neighbor of schedules.

2. Dynamic frequency-selection.

We developed a new DFS algorithm for CR application. The new DFS algorithm utilizes all relevent environmental information, including data history, current measurement, and future prediction. In this DFS algorithm, we adopt the Gaussian mixture model to approximate traffic patterns of primary users. The K-means algorithm is applied for parameter initialization, and the Expectation maximization algorithm is used for parameter learning. The new DFS algorithm effectively reduces the collision probability between CR users and primary users.

3. Transmit-power control

In the CR mesh network, the TPC uses the iterative water-filling algorithm, which was originally introduced in digital-subscriber-line systems. We modified the original IWF algorithm to avoid the dropping of link, caused by the transmit-power adjustment in the mesh network. Simulation results show that the modified IWF algorithm is able to protect the performance of pre-existing links when a new link is added to the network. Compared with the original IWF algorithm, the number of iterations required for a new link establishment is almost unchanged using the modified IWF algorithm, while the subtle adjustment time of the network is prolonged.

Although indeed there is much that needs to be uncovered about cognitive radio, nevertheless, through the contributions summarized above, it can be said that we have made a “dent” in this new and highly exciting area of wireless communications.

Appendix A

Program List

1. **Chapter 2**

   - main.m: The simulation entry and timer setting.
   - Transceiver: Physical layer timer processing.
   - TransceiverActive.m: MAC layer timer processing.
   - NodeEntry.m: The new node entry processing.
   - MeshElection.m: sponsor node selection
   - NENTProcess.m: sponsor node processing
   - NodePolling.m: Node control signal generating procedure.
   - NetworkUpdate.m: The network topology update because of node state change.
   - CalculateSS.m: The random subscribe station position and frequency offset setting.
   - network_topology.m: The topology change caused by the input.
   - changeSS: The SS state modification I/O processing.
   - ChannelPass: AWGN channel generation
   - contourSS.m: The neighbourhood contour calculation.

- ControlChannelProcess.m: Control channel signalling processing.
- DrawNeighbor.m: The linkage state display.
- GainNeighbor.m: channel attenuation calculation with shadow fading.
- LinePolling: Tx physical layer processing.
- txphy.mdl: Simulink model of transmit path.
- LinkEntry: Rx physical layer processing.
- cordic.c: The iterative algorithm for calculating sine and cosine value, and the rotation for FFT algorithm.
- fft.c: The radix-4 fft algorithm.
- fftmodule.c: The radix-2 fft algorithm including pre-fft and post-fft for real-complex exchanging.
- rstest.c: RS code test routine.
- RS_ENC.c: The encoder procedure of Reed-Solomon codeword.
- RS_DEC.c: The decoder procedure of Reed-Solomon codeword, including Syndrome calculation, Berlekamp-Massey, Chien search and Forney algorithms.
- OFDMmapping.m/OFDMdemapping.m: The channel allocation in OFDMA mode for generating the block module.
- interleaver.m/deinterleaver.m: The block interleave/deinterleave procedure for generating the block module.
- IEEE80216aOFDMA.mdl: The Simulink module for the physical layer realization of 802.16a OFDMA mode.

2. **Chapter 3**

- gmminit.m

- EM_init.m: EM algorithm initialization procedure
- EM_learn.m: EM iterative learning procedure
- observation_likelihood.m: Observation likelihood calculation
- log_Likelihood.m: Log-likelihood of the GMM
- gaussian_prob1.m: Gaussian probability
- gausspdf1.m: Gaussian distribution PDF
- mgaussv1.m: The interface
- FBmix.m: forward-backward calculation
- gmminit.m: initialization of GMM
- GMM_EM.m: $3 * k$ parameters learning
- EMtest.m: the test module of the algorithm
- CSMA0.m: CSMA/CA traffic analysis
- WLANEnviron.mdl: Simulink model of the simulation environment
- M_M_1.m: the M/M/1 model
- M_G_1.m: the M/G/1 model
- G_G_1.m: the G/G/1 model
- SegGroup.m: segment and grouping model of the environment analyzer
- Collision2.m: CR simulation using DFS with traffic analysis
- Collision3.m: CR simulation using DFS with RSS only
- statisgreedy.m: control of random runs of DFS algorithms to get the average result

3. **Chapter 4**

- waterfilling.m: the greedy water-filling algorithm.

- checkwaterfilling.m: check the rate requirement with 6dB margin.
- waterfillings.m: water-filling with rate requirement only.
- checkwaterfillingS.m: the rate check with 4dB margin.
- TPCssDisplay.m: the neighborhood display.
- TPCSS.m: the transmit power control in the mesh network.
- nodeTPC.mat: the mesh network result from chapter 2.
- TPCSS_org_count1.m: The statistic analysis of original IWA
- TPCSS_new_count1.m: The statistic analysis of modified IWA
- TPCSS_org_count2.m: The power and channel usage result of original IWA
- TPCSS_new_count2.m: The power and channel usage result of modified IWA
- TPCSS_org.m: The stable status before a special link establishment
- TPCSS1.m: The example of a special link establish procedure of original IWA
- TPCSS2.m: The example of a special link establish procedure of modified IWA
- CheckPowerDeficit.m: The power deficit estimation

Bibliography

Akyildiz, I., Wang, X., and Wang, W. 2005. "Wireless mesh networks: a survey", *Computer Networks.* http://www.ece.gatech.edu/research/labs/bwn/mesh.pdf.

Bharghavan, V., Demers, A., Shenker, S., and Zhang, L. 1994. MACAW: A media access protocol for wireless LANs, *Proc. ACM SIGCOMM'94*, 212.

Bingham, J. A. C. 2000. *ADSL, VDSL, and Multicarrier Modulationm.* John Wiley & Sone.

Blogh, J. S., Cherriman, P. J., and Hanzo, L. 2001a. Comparative study of adaptive beam-steering and adaptive modulation-assisted dynamic channel allocation algorithms, *IEEE Transactions on Vehicular Technology*, 50, 398.

Blogh, J. S., Cherriman, P. J., and Hanzo, L. 2001b. Dynamic channel allocation techniques using adaptive modulation and adaptive antennas, *IEEE Journal on Selected Areas in Communications*, 19, 312.

Busch, P. and Malhotra, R. 2002. Wireless LAN with channel swapping between DFS access points. US patent application number: 20020176437.

Colvin, A. 1983. CSMA with collision avoidance, *Computer Commun.*, 6, 227.

Cooper, C. W. R., Zeidler, J. R., and Bitmead, R. R. 2004. Modeling dynamic channel-allocation algorithms in multi-BS TDD wireless networks with internet-based traffic, *IEEE Transactions on Vehicular Technology*, 53, 783.

Cowen-Hirsch, R. 2000. Software radio: Evolution or revolution in spectrum management, *MILCOM 2000, 21st century military communications conference proceedings.*

Cuomo, F., Martello, C., and A.Baiocchi 2002. Radio resource sharing for ad-hoc networking with UWB, *IEEE Journal on Selected Areas in Communications*, 20, 1722.

FCC 2002. Spectrum Policy Task Force Report. ET Docket No. 02-135.

FCC 2003. NOTICE OF PROPOSED RULEMAKING AND ORDER Facilitating Opportunities for Flexible, Efficient, and Reliable Spectrum Use Employing Cognitive Radio Technologies. FCC 03-322.

Feng, N., Mau, S.-C., and Mandayam, N. B. 2004. Pricing and power control for joint network-centric and user-centric radio resource management, *IEEE Trans on Commun*, 52, 1547.

Fette, B. 2003a. Cognitive radios. Cognitive Radio Workshop Presentations.

Fette, B. 2003b. Cognitive radios the next step for SDR. EE Times.

Floroiu, J., R., R., Sisalem, D., and Voglimacci, J. 2003. Seamless handover in terrestrial radio access networks: a case study, *IEEE Communications Magazine*, 41, 110.

Fong, B. and et. al. 2004. On the scalability of fixed broadband wireless access network deployment, *IEEE Communications Magazine*, 42.

Goldsmith, A. 2005. *Wireless Communications.* Online.

Grossglauser, M. and Tse, D. 2002. Mobility increases the capacity of ad hoc wireless networks, *Networking, IEEE/ACM Transactions on.*

Gupta, P. and Kumar, P. 2000. The capacity of wireless networks, *IEEE Transactions on Information Theory*, 46, 388.

Gupta, P. and Kumar, P. R. 2001. Internets in the sky: The capacity of three dimensional wireless networks, *Communications in Information and Systems*, 1, 33.

Haas, Z. and Deng, J. 2002. Dual busy tone multiple access (DBTMA)a multiple access control scheme for ad hoc networks, *IEEE Trans. Commun*, 50, 975.

Haykin, S. 2005. Cognitive radio: brain-empowered wireless communications, *IEEE JSAC*, 23, 201.

Haykin, S. and Moher, M. 2004. *Modern Wireless Communications.* Prentice-Hall.

IEEE802.11 1999. LAN/MAN Specific Requirements - Part 11: Wireless Medium Access Control (MAC) and physical layer (PHY) specifications: High Speed Physical Layer in the 5 GHz band, , 5.

IEEE802.16 2003. Local and Metropolitan Area Networks - Part 16: Air Interface for Fixed Broadband Wireless Access Systems Amendment 2 - Medium Access Control Modifications and Additional Physical Layer Specifications for 2-11GHz, , 3.

Jiang, L., Wiklund, K., and Haykin, S. 2005. A Simulink laboratory package for teaching adaptive filtering concepts, *The international journal of engineering education.* To be published.

Johnson, D. and Maltz, D. 1996. *Dynamic source routing in ad hoc wireless networks.* Mobile Computing, edited by T. Imielinski and H. Korth, chapter 5.

Jun, J. and Sichitiu, M. 2003. The nominal capacity of wireless mesh networks, *IEEE Wireless Communications*, 10, 8.

Karn, P. 1990. MACA - A new channel access method for packet radio, *ARRL/CRRL Amateur Radio 9th Computer Networking Conference*, 134.

Kawadia, V. and Kumar, P. R. 2005. Principles and protocols for power control in wireless ad hoc networks, *IEEE JSAC, special issues on wireless ad hoc networks*, 23, 76.

Kim, K., Kim, H., Han, Y., and Kim, S.-L. 2004. Iterative and greedy resource allocation in an uplink OFDMA system, *Personal, Indoor and Mobile Radio Communications, 2004. PIMRC 2004. 15th IEEE International Symposium on*, 4, 2377.

Li, J., Haas, Z., Sheng, M., and Chen, Y. 2003. Performance evaluation of modified IEEE 802.11 MAC for multi-channel multi-hop ad hoc networks, *Journal of Interconnection Networks*, 4, 345.

Liu, K., Li, J., yu Huang, P., and Fukuda, A. 2002. Adaptive acquisition multiple access protocol in wireless multihop mobile ad hoc networks, *Proceedings of VTC 2002 Spring*.

Marsic, I. 2003. *Chapter 3: Wireless network.* Telecommunication Networks Online materials: course lecture notes. http://www.caip.rutgers.edu/ marsic/book-mobicomp/ch3-WN.pdf.

McFarland, W. J. and Green, M. R. 2003. Methods for implementing a dynamic frequency selection (DFS) and a temporary channel selection feature for WLAN devices. http://www.uspto.gov/web/patents/patog/week12/OG/html/1292-4/US06870815-20050322.html.

Mclachlan, G. J. and Basford, K. E. 1992. *Mixture Models - Inference and Applications to clustering.* Dekker.

Medidi, M. and Daptardar, A. 2004. A distributed algorithm for mesh scatternet formation in bluetooth networks, *ICWN'04*, 22.

Mills, D. 1983. RFC 889: Internet Delay Experiments, *Good stuff IT services.* http://www.good-stuff.co.uk/useful/rfc.php?rfc=889.

Mitola, J. 1999. Software radio architecture: a mathematical perspective, *IEEE journal on selected area of communications*, 17, 514.

Mitola, J. 2000. *Cognitive Radio: An Integrated Agent Architecture for Software Defined Radio.* Dissertation, Doctor of Technology, Royal Institute of Technology (KTH),Sweden.

Moose, P. 1994. A technique for orthogonal frequency division multiplexing frequency offset correction, *IEEE Trans. on Comm.*, 42, 2908.

Nokia 2002. Nokia Supplementary Response to UK Radiocommunications Agency 5GHz consultation - Fixed Wireless Access at 5GHz Spectrum Co-existence Study. http://www.ofcom.org.uk/static/archive/ra/topics/mobiledata /consult/5ghz/responses/nokiasupplement.doc.

Nynamics, M. 2004. CHALLENGES FOR 802.15 WPAN MESH. http://www.meshdynamics.com/Publications/MDWPANOVERVIEW.pdf.

Pearlman, M. and Haas, Z. 1999. Determining the optimal configuration for the zone routing protocol, *IEEE Journal on Selected Areas in Communications, Special Issue on Wireless Ad Hoc Networks*, 17.

Perkins, C. E. 2001. Performance comparison of two on-demand routing protocols for ad hoc networks, *IEEE Personal Communications*, 8, 16.

Petrushin, V. A. 2000. Hidden markov models: fundamentals and applications, *Online Symposium for Electronics Engineer.* www.accenture.com/xdoc/en/services/technology/publications/hmmtutorialpart2.pdf.

Resch, B. 2004. Mixtures of Gaussians: A Tutorial for the Course Computational Intelligence. http://www.igi.tugraz.at/lehre/CI.

Ritter, M., Friday, R. J., Garces, R., Filippo, W. S., Nguyen, C.-T., and Srivastava, A. Mobile connectivity protocols and throughput measurements in the Ricochet microcellular data network (MCDN) system, *SIGCOMM 2001.*

Schollmeier, R., Gruber, I., and Finkenzeller, M. 2002. Routing in mobile ad-hoc and peer-to-peer networks. A comparison, *International Workshop on Peer-to-Peer Computing.*

Shepard, T. 1995. *Decentralized Channel Management in Scalable Multihop Spread-Spectrum Packet Radio Networks.* Ph.D. Thesis, MIT.

Stallings, W. 2004. *Data and Computer Communications 7th edition.* Prentice-Hall Inc.

van de Beek, Borjesson, Boucheret, Landstrom, Arenas, Ostberg, Wahlqvist, and Wilson 1999. A time and frequency synchronization scheme for multiuser OFDM, *IEEE JSAC*, 17, 1900.

Wong, C., Cheng, R., Letaief, K., and Murch, R. 1999. Multiuser OFDM with adaptive subcarrier, bit and power allocation, *IEEE JSAC*, 17, 1747.

Yaghoobi, H. 2004. Scalable OFDMA Physical Layer in IEEE 802.16 WirelessMAN, *Intel Technology Journal*, 8. http://www.intel.com/technology/itj/2004/volume08issue03 /art03_scalableofdma/p03_multicarrier.htm.

Yu, W. 2002. *Competition and Cooperation in Multiuser Communication Environments.* Ph.D. thesis, Stanford University.

Zhao, D. 2004. *ECE739 course notes.*